Review

A Review of Water Management in Polymer Electrolyte Membrane Fuel Cells

Mengbo Ji and Zidong Wei *

State Key Laboratory of Power Transmission Equipment & System Security and New Technology, School of Chemistry and Chemical Engineering, Chongqing University, Chongqing, 400044, China; E-Mail: mbji@cqu.edu.cn

* Author to whom correspondence should be addressed; E-Mail: zdwei@cqu.edu.cn; Tel.: +86 23 60891548; Fax: +86 23 65106253.

Abstract: At present, despite the great advances in polymer electrolyte membrane fuel cell (PEMFC) technology over the past two decades through intensive research and development activities, their large-scale commercialization is still hampered by their higher materials cost and lower reliability and durability. In this review, water management is given special consideration. Water management is of vital importance to achieve maximum performance and durability from PEMFCs. On the one hand, to maintain good proton conductivity, the relative humidity of inlet gases is typically held at a large value to ensure that the membrane remains fully hydrated. On the other hand, the pores of the catalyst layer (CL) and the gas diffusion layer (GDL) are frequently flooded by excessive liquid water, resulting in a higher mass transport resistance. Thus, a subtle equilibrium has to be maintained between membrane drying and liquid water flooding to prevent fuel cell degradation and guarantee a high performance level, which is the essential problem of water management. This paper presents a comprehensive review of the state-of-the-art studies of water management, including the experimental methods and modeling and simulation for the characterization of water management and the water management strategies. As one important aspect of water management, water flooding has been extensively studied during the last two decades. Herein, the causes, detection, effects on cell performance and mitigation strategies of water flooding are overviewed in detail. In the end of the paper the emphasis is given to: (i) the delicate equilibrium of membrane drying *vs.* water flooding in water management; (ii) determining which phenomenon is principally responsible for the deterioration of the PEMFC performance, the flooding of the porous electrode or the gas

channels in the bipolar plate, and (iii) what measures should be taken to prevent water flooding from happening in PEMFCs.

Keywords: polymer electrolyte membrane fuel cells (PEMFCs); water management; water flooding; membrane drying; catalyst layer(CL); flow channel

1. Introduction

Polymer electrolyte membrane fuel cells (PEMFCs) are considered a possible answer to environmental and energy problems, and are expected to soon become the most promising energy converters for automotive, stationary, and portable applications, because of their high-energy density at low operating temperatures, quick start-up and zero emissions. Consequently PEMFCs have increasingly been cited by governments as a possible pathway to the reduction of greenhouse gas emissions [1]. Figure 1 shows a schematic of a PEMFC and the processes happening during PEMFC operation. The operating principle of a PEMFC is as follows: at the anode, fuel H_2 is oxidized liberating electrons and producing protons. The electrons and protons flow via the external circuit and via proton exchange membrane inserted tightly between the anode and the cathode, respectively, to the cathode, where they combine with the dissolved oxidant O_2 to produce water and heat.

Figure 1. Schematic picture of the operating principle of a typical PEMFC.
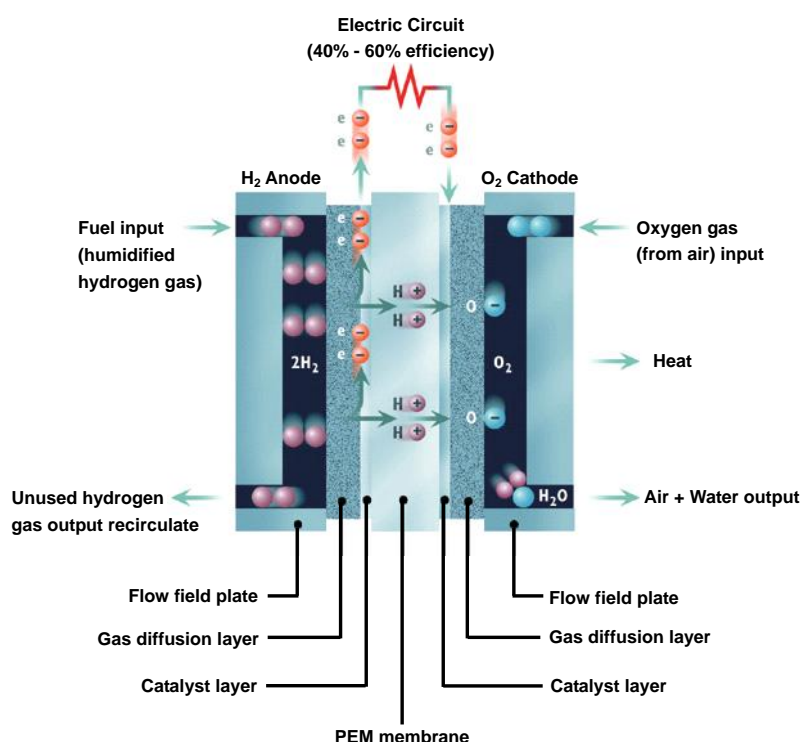
Obviously, it is important to optimize the thermal and water management. Thermal management is required to remove the heat and prevent overheating and dehydration of the membrane. Proper water

management is also important. Recent studies have shown that water management is of vital importance to achieve maximum performance and durability from PEMFCs [2,3]. On the one hand, to maintain good proton conductivity and hence performance, the relative humidity of the inlet gases is typically held at a large value to ensure that the membrane remains fully hydrated. On the other hand, the pores of the catalyst layer (CL) and the gas diffusion layer (GDL), as well as gas flow channels may be flooded by excessive liquid water, resulting in a higher mass transport resistance. Thus, a subtle equilibrium has to be maintained between membrane drying and liquid water flooding to prevent fuel cell degradation and guarantee a high performance level. This is the key to water management in PEMFCs.

The purpose of the present review is to summarize the state-of-the-art studies of water management. It covers: (1) a brief introduction to the general issues of water management, where the stated focus is placed on the water transport in PEMFCs; (2) the consequences of flooding or drying caused by improper water management; (3) the experimental diagnosis and measurement of water management; (4) the mathematical models and experiments related to water management; (5) the water management strategies; and finally (6) a survey of prospects in future water management studies.

2. General Issues of Water Management

As shown in Figure 1, a single PEMFC consists of a membrane electrode assembly (MEA) sandwiched between gas diffusion layers and flow field plates into which gas channels have been machined. The MEA comprises two electrodes, anode and cathode, which are separated by a gas tight, proton conducting membrane. At the anodic membrane-electrode interface, hydrogen is oxidized electrochemically and the resulting protons are conducted through the membrane. At the cathodic membrane–electrode interface, oxygen is reduced electrochemically, yielding water as product. The product water is transported along the gas channels as well as in the direction perpendicular to the MEA (Figure 2).

Figure 2. The water transport mechanism inside a PEMFC.
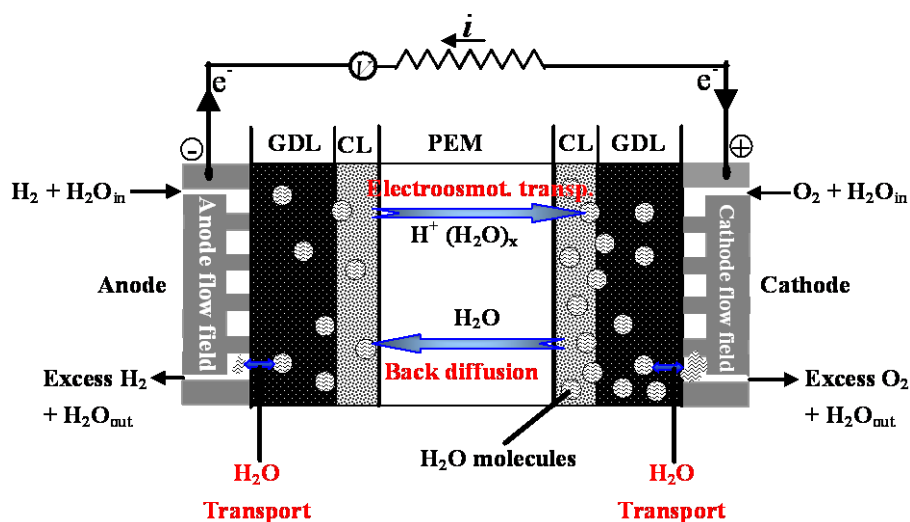
In addition, protons are surrounded by a certain amount of water molecules. Thus, when a current is drawn from the fuel cell protons migrate through the membrane. Depending on the hydration state of

the membrane, proton migration is associated with a drag of water molecules from the anode to the cathode side, as shown in Figure 2. This so-called "electro-osmotic drag" transport [4-6], together with electrochemical water production, results in an accumulation of water at the cathode side. In turn, the water concentration gradient between the anode and cathode causes back diffusion, which works against drying of the membrane from the anode side. The gradient between anodic and cathodic water concentration is determined by the thickness of the membrane, its water content and humidity of the reactant gases. The latter in turn is dependent on the gas inlet humidification and on the temperature and pressure in the gas channels [7]. Besides, at low current densities, back diffusion will prevail on electro-osmotic drag, while at high current densities, electro-osmotic drag will prevail over back diffusion and thus the anode will tend to dry out, even if the cathode is well hydrated [8].

Thus, there is an inherent contradiction in the operation of a PEMFC system. On the one hand, water is needed to guarantee good proton conductivity in the ionomer phase of the proton exchange membrane, because protons move in the hydrated parts of the ionomer via dissociation of sulfonic acid bonds [9]. Therefore, in a dry ionomer phase, where the sulfonic acid bond cannot be dissociated, the protons cannot migrate, leading to the decrease of ionic conductivity. Furthermore, a low ionic conductivity hinders the access of protons to the catalyst surface, decreasing the actual number of reactive active sites in the catalyst layer, thus increasing the activation polarization [10]. In addition, severe drying conditions can lead to irreversible membrane degradations (such as delamination, pinholes) within about 100 s [11,12]. As a result, the ohmic resistance of the whole cell system will increase remarkably. On the contrary, a fully hydrated membrane can achieve ca. 300 times higher conductivity than a dry one [13]. Hence, maintaining a high water content in the electrolyte is fundamental to ensure high ionic conductivity.

On the other hand, the presence and accumulation of liquid water in the flow-field channels and/or electrodes gas porosities must be transported away from the catalyst layer by evaporation, water–vapor diffusion and capillary transport of liquid water through the gas diffusion layer (GDL) into the flow channels of the flow field, and then exhausted out of the system, or else excess water will block the flow channels or/and the pores of the GDL and catalyst layer (CL) and then reducing the catalyst active sites of the CL. This phenomenon is known as "flooding", and is an important limiting factor of PEM fuel cell performance. Generally, flooding of an electrode is linked to high current density operation that results in the water production rate greater than the removal rate. However, even so, the extent of flooding and the effects of flooding strongly depend upon the interaction of the operating conditions, particularly under low gas flow rates/temperature levels [14] or if liquid water is not removed from the channels in time [15,16], and the MEA properties. Moreover, even if liquid water floods both electrodes [17,18], the flooding at the cathode catalyst layer is especially crucial where water is produced by the oxygen reduction reaction (ORR) [19]. The accumulation of the liquid water in the channels is observed only after the complete saturation of the gas with water vapor because the evaporation and water vapor transport are relatively faster than liquid water transport (generally by capillary mechanism within the GDL, or the drag force exerted by the convective flow of the gas near the channels) [18]. Furthermore, once the channels flooding, the evacuation of liquid water from the electrode is decreased because of the water evacuation towards the channels decreases due to the water saturation gradient decrease. On the other hand, the flooding in the GDL and the CL likely occurs prior

to that in the gas channels, because the water is produced in the CL and then expelled through the GDL to the flow channels [20]. Besides, flooding can also occur even at low current densities under certain operating conditions, such as low temperatures and high gas relative humidity [21] as well as low gas flow rates, where faster saturation of the gas phase by water–vapor [22] can occur. In general, most of the consequences of a short-term flooding are reversible [23], but, more than 30 min were needed to reach a new steady state when subjected to current-density changes owing to the slow liquid water transport process [24]. Moreover, a long-term operation under excess liquid water may lead both to mechanical degradation of the MEA's material and to local fuel and oxidant starvation [23].

Besides, under freezing conditions, the water may solidify into ice; care must be taken to prevent that phase transformation from destroying the integrity of the cell. Thus, water in PEMFC acts as a "lubricant" making the cell run smoothly. Too much water drowns the cell and makes it function inefficiently; too little dehydrates it [25]. Therefore, how to find a subtle equilibrium between membrane drying and liquid water flooding is significantly critical to guarantee a high performance of PEMFC [26,27]. Especially in a fuel cell stack with series connected single cells, operating conditions may vary significantly not only in the plane of the MEA but also along the stack axis. For example, an even fluid distribution to all the individual cells and a homogeneous temperature distribution are difficult to achieve [28]. Due to the fact that these operating parameters directly affect water management, it is an even more challenging task to maintain a proper water balance in a fuel cell stack than in a single cell alone [29].

3. Influence of Water Management on Fuel Cell Performance and Life

According to the above discussion, improper water management can lead to membrane dehydration and electrodes flooding. Then, the question becomes what adverse impact on fuel cell performance and life can be brought about by the two cases?

### 3.1. Membrane Dehydration

Dehydration of the membrane is more likely to occur at the anode side of the membrane. Three main reasons may cause membrane dehydration, as follows: (1) sufficient humidification cannot be maintained when feeding the cell with low-humidified or dry reactant gas streams; (2) water formation reaction at the cathode alone is not able to compensate the lack of water, especially at higher cell operating temperatures; (3) electro-osmotic drag can also lead to dehydrated condition at the anode. As mentioned above, at high current densities the water replenishment by back-diffusion is not sufficient to keep the anode side of the membrane hydrated [30]. In a case of a step increase of the current density the electro-osmotic force will immediately pull water molecules from the anode to the cathode [31]. In addition, anode dehydration should be more serious at the inlet of the cell because of the higher water back-diffusion to the anode at the outlet of the cell, which is not difficult to understand since the water content at the outlet of the cathode is higher resulted from water draining, the back-diffusion is higher as well [32]. Moreover, under the dehydrated condition the membrane pores will shrink, leading to lower back-diffusion rates. During operation this effect can be aggravated by poor thermal management [33].

The main consequence of dehydration is drying of the proton-exchange-membrane. With a decrease in water content the conductivity decreases, leading to higher ionic resistance and larger ohmic losses [2,13], which results in a substantial drop in cell potential and thus a temporary power loss [2,31,33]. Büchi and Srinivasan [34] confirmed a long-term MEA performance degradation under operation conditions of zero external humidification: after 1,200 h life-tests the current density dropped from 170 to 130 mA cm^{-2} at a constant potential of 0.61 V. A temporary drop in voltage can usually be recovered by humidification, and the recovery time depends on the membrane thickness and the water diffusion coefficient [2,31]. However, dry cell operation over a long time can cause serious and irreversible damage to the membrane, *i.e.*, they can become brittle and develop crazes or cracks, which cause gas crossover and therefore uncontrolled reaction of H_2 and O_2 leading to formation of hot spots [35]. Hot spots are high chemically active areas on the membrane caused by the exothermic reaction of H_2 and O_2, which in turn causes pinholes, resulting in more gas crossover. Once this process is initiated, a "destructive cycle" of increasing gas crossover and pinhole production is established [36]. Generally, the drier the operating conditions, the shorter will be the life of the cell [30].

3.2. Fuel Cell Flooding

Water flooding is the accumulation of excess water and can happen at both the anode and cathode side of the membrane. Flooding leads to instant increase in mass transport losses, particularly at the cathode. The transport rate of the reactants to the catalyst active sites is significantly reduced [24]. Excess water blocks the pores of the GDL and thus prevents the reactants from reaching the catalysts' active sites, leading to gas starvation and an immediate drop in cell potential (current). The time-dependent oscillation of cell current density at fixed voltage (0.6 V), as shown in Figure 3, represents a typical flooding pattern in a PEM fuel cell as observed in our laboratory.

Figure 3. A typical water flooding pattern in a PEM fuel cell operated at constant cell voltage (0.6 V).
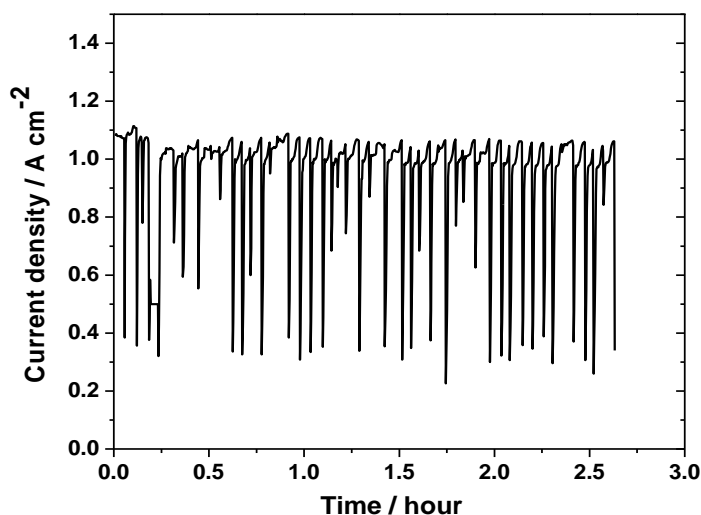
When the operating conditions allow the liquid water to accumulate to some extent and severe water flooding occurs, the gas flow path can be temporarily blocked, giving rise to a sharp reduction in current density; then the blocking of the gas flow path can result in a sudden build-up of local pressure

that quickly flushes out the excess liquid water, thereby resulting in a quick restoration of the current density. The periodic build-up and removal of liquid water in the cell causes the observed fluctuation in the cell performance, causing unstable, unreliable and inconsistent cell performance [27]. In addition, water flooding not only compromises the cell performance in a transitory manner but also degrades the durability of the fuel cell [23].

3.2.1. Cathode flooding

The general consensus is that water flooding is more prone to occur at the cathode, owing to the following three mechanisms: (1) Water formation due to the ORR generates water. There will be more water generated with the increase of the load or the current density. (2) Under the influence of an applied electric field across the membrane the electro-osmotic drag pulls water molecules as the along with protons from the anode to the cathode. The rate of transported water depends on the humidification level of the membrane and increases with increasing current density [33]. (3) Over-humidified reactant gases and liquid water injection also lead to flooding.

The water accumulated in the cathode is usually removed out of the porous electrode via evaporation, water–vapor diffusion and capillary transport through GDL into the flow channels or by water back-diffusion trough membrane to the anode. The latter does not contribute much to water removal, because only at lower current densities (less than 0.3 A cm^{-2}) there is a possibility that back diffusion can prevail on electro-osmotic drag leading to the net water transport toward to anode [33]. However, cathode flooding is more prone to occur at higher current densities accompanied by the fact that electro-osmotic drag excesses back diffusion [8], resulting in an increase in the water content in the cathode. As a result, the cathode flooding is aggravated further. The water removal via evaporation and water–vapor diffusion generally take place at higher cell operation temperature and a higher air flow rate, when a decrease in surface tension and viscosity of water makes it easier to flush water out of the cell [24].

Once the accumulated water cannot be removed out of cathode efficiently, the water flooding will bring a negative effect on fuel cell performance, as shown in Figure 4. For example, at higher current densities (above 0.55 A cm^{-2}) the partial-gas-pressure-drop at the cathode due to flooding increases significantly which results in a considerable cell voltage drop. Furthermore, if the cathode pressure drop doubles from 1.5 kPa to around 3 kPa, the initial cell voltage of 0.9 V goes down to around one third of its initial value [24].

In addition, with water accumulation and the cathode flooded, oxygen ingress into the catalyst surface will be hindered [22,37,38]. The lack of oxygen reaching the catalyst leads to oxygen under-stoichiometry or "starvation" at the cathode [39]. Under steady state conditions, the net mass flow rate of oxygen into the system is equal to the oxygen consumed by the electrochemical reaction. In transient conditions, in particular a sudden increase in power requirement from the fuel cell, oxidant supply to the system lags behind the demand and causes a shortage of oxygen and local oxygen starvation for the reaction thus increasing oxygen concentration overpotential at the cathode. Worse still, proton (H^+) reduction reaction (PRR), instead of ORR would occur at the cathode if oxygen were depleted at the cathode.

Figure 4. Effect of cathode flooding on a PEM fuel-cell performance (cell temperature: 51 ℃; H$_2$ flow rate: 2.0 A cm^{-2}; air flow rate: 2.8 A cm^{-2}; ambient pressure; H$_2$ sparger temperature: 50 ℃; air sparger temperature: 27 ℃) [24].
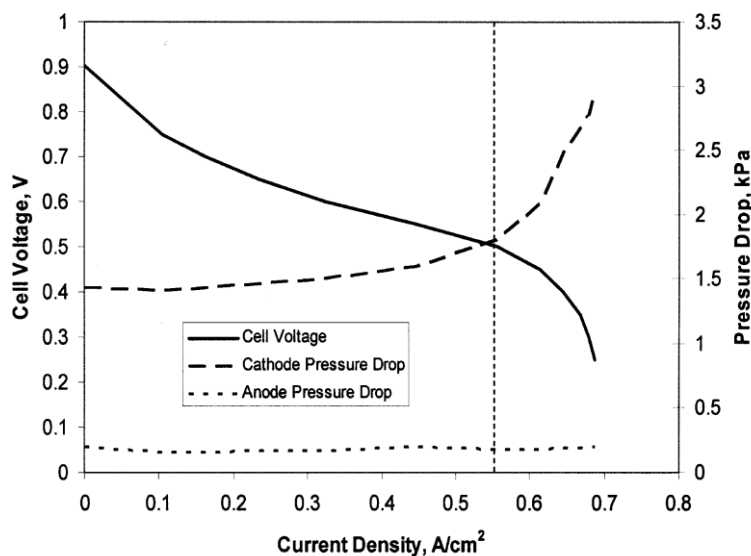

In the case of oxygen starvation, the original electron consuming process ORR:

$$O_2 + 4H^+ + 4e^- = 2H_2O \ (E^0 = 1.23V) \tag{1}$$
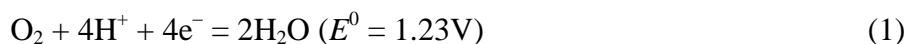
would be replaced by the new electron consuming process, PRR:

$$2H_3O^+ + 2e^- = H_2 + 2H_2O \ (E^0 = 0.00V) \tag{2}$$
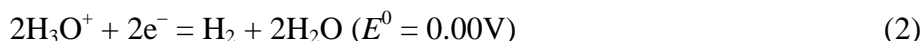
In this case, the cathode potential would drop from 1.23 V to 0.00 V at current off and probably from 0.8 V to –0.1 V at current on with substitution of PRR for the ORR. Electrode polarization occurs with current flowing through the electrode. The cathode polarization causes potential shift toward the negative direction but anode polarization toward the positive direction. For hydrogen oxidation reaction (HOR) taking place at the anode:

$$H_2 + 2H_2O = 2H_3O^+ + 2e^- \ (E^0 = 0.00V) \tag{3}$$
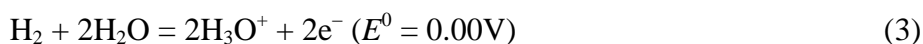
with current flowing, electrode potential will shift toward the positive direction, for example, 0.1 V. Thus, the cell voltage would change from original 0.7 V by (0.8–0.1) to –0.2 V by (–0.1–0.1) as shown in Figure 5. The output voltage of the cell, which is under oxygen starvation, would be likely reversed from a positive value, for instance 0.7 V, to a negative value, for instance –0.2 V, with substitution of PRR for the ORR. This phenomenon is known as the voltage reversal effect (VRE) in a PEMFC [40,41]. In a stack of PEMFCs, when VRE happens in a single cell not only does it not contribute to the performance output of the whole stack, but also can counteract partial effective output voltage from other single cell. Therefore, as long as the VRE appears, the output of the stack will be seriously impaired.

Figure 5. The formation of voltage reversal effect (VRE) in a PEMFC.
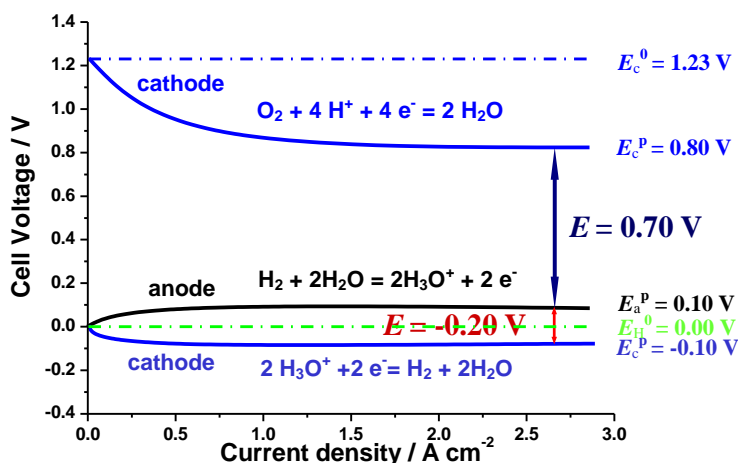
3.2.2. Anode flooding

Although flooding at the anode happens less often than at the cathode, low hydrogen flow rates can make more liquid water stay in the anode leading to fuel starvation and thus the serious decline of fuel cell performance. Usually, the following several operation conditions will cause anode flooding: (1) lower current densities and lower cell temperatures. Wang [14,42] confirmed that anode flooding is often observed at low current densities (0.2 A cm^{-2}), especially at low reactant flow rates and lower temperatures. (2) Anode flooding can also be caused by water back-diffusion from the cathode together with a low hydration state of the fuel gas stream [33]. At low current densities, if the relative humidity is not as high as at the cathode, water back-diffusion through the GDL to the anode will surpass the electro-osmotic drag effect leading to the increase of water content in the anode, especially at the exit. (3) Liquid water injection for cooling and humidification together with moderate cell temperatures (lower evaporation) can lead to the water accumulation in the anode and hence the anode flooding [33,42,43]. As the result, anode flooding in a single cell within a fuel cell stack could lead to not only fuel starvation and carbon substrate oxidation but also oxygen evolution.

3.2.3. Flow channels flooding

It has to be noted that flooding occurs not only in the porous electrodes themselves of the cathode and anode, but in the gas flow channels of the flow field as well, depending on the interplay of the properties and engineering of those components, and the operating conditions. Flow channels flooding can also hinder the reactant gas ingress to the porous electrodes and impair the power output of the fuel cell. Besides, when multiple parallel channels are used flow channels flooding in one of the channels could lead to starved regions with multiple consequences.

Besides output voltage losses of an operating PEM fuel cell, water flooding can also cause changes in the characteristic properties, such as: (1) water condensation in a local site leads to a locally lower current density owing to water-hindered gas transport; (2) a locally elevated temperature leaded by the released enthalpy of the condensing water could cause an uneven local distribution of current density and temperature; and (3) the accumulation of liquid water in GDL or in the flow channels leads to the

gas flow resistance to rise, which in turn results in an increase in the pressure drop between the inlet and outlet of the fuel cell [17,24,27].

4. Visualization of Liquid Water Distribution

In order to evaluate the effectiveness of water management schemes, methods capable of looking inside an operational fuel cell and visualizing the distribution of liquid water could be very useful. These visualization techniques mainly include direct visualization, nuclear magnetic resonance (NMR) imaging, beam interrogation, and fluorescence microscopy. Among these techniques, the direct visualization has the advantage of providing high temporal and spatial resolution information about water transport in the gas flow channels [15,16,42,44-55], the smaller scale of the GDL pores [56-64] and the micro-scale of the catalyst surface [21] in an operating fuel cell. Because of the opaque nature of traditional GDL and bipolar plate materials, the investigation and diagnosis of liquid water transport dynamic in an operating PEM fuel cell is a challenging phenomenon using *in situ* visualization techniques. However, NMR imaging [65-79] and beam interrogation techniques, such as neutron imaging [80-106], electron microscopy [107-110], and X-ray techniques [111-116], enable the *in situ* measurement of liquid water distributions in operating PEM fuel cells through materials that would otherwise be opaque to optical access [117]. Using fluorescence microscopy [57,61,118], liquid water can be detected in the through plane direction of the GDL, but limited in depth to several fiber diameters due to the opacity of the material [57].

4.1. Direct Visualization

Direct visualization techniques require a transparent cell plate that allows access to the channels for optical devices, including digital camcorders and high-speed cameras [21,49], infrared cameras [50] and CCD cameras [43,56]. By using these methods, their spatial and temporal resolution are only limited by the employed microscope magnification and camera speed, respectively [117]. It is especially useful to directly observe the effects of operating conditions on water droplet formation, growth and movement [42,49,51,58,59]. For example, Wang and Hussaini [47] characterized channel flooding and liquid water coverage on cathode GDL by *in situ* visualization of cathode flooding in an operating fuel cell with a cathode side covered by a transparent Lexan plate providing a clear view of the channels. They found that two-phase transport in fuel cell micro-channels occurs principally in the form of droplet, film and slug-flow with the two-phase region being preceded by a single-phase region. The actual images corresponding to these flow patterns are given in Figure 6. A simulated flow channel apparatus [53] was employed to study the effects of hydrophobicity, channel geometry, droplet chord length and height, and air flow rate on droplet formation and instability. Meanwhile, an analytical force balance model was also presented to predict the droplet characteristics at instability [53]. On the other hand, the effect of GDL materials and their hydrophobicity on the liquid water transport was studied [21,49,64].

Figure 6. Magnified view of flow patterns in channels and their corresponding line illustrations showing the form and distribution of liquid water [47].
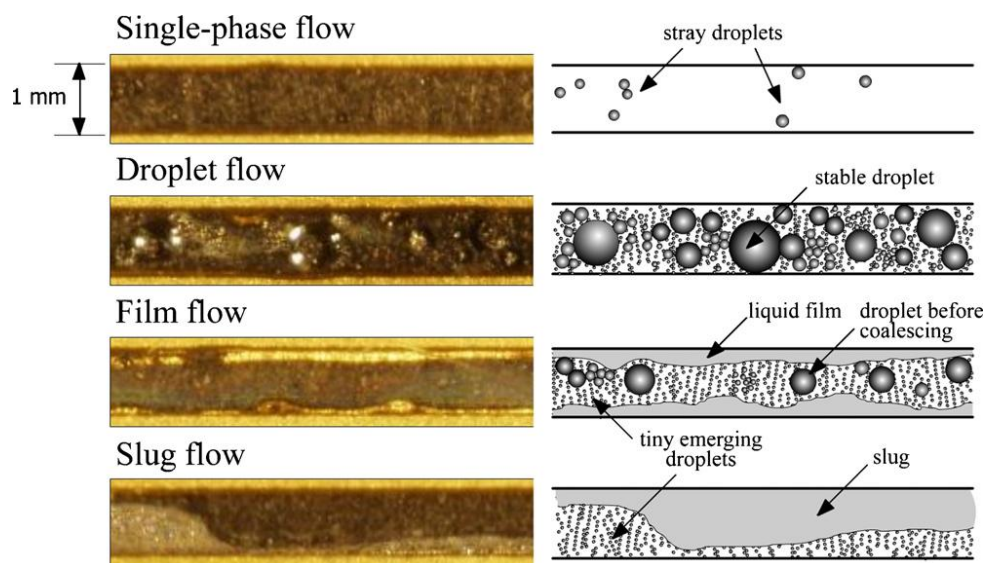
Besides, López *et al*. [44] verified that saturated condition for the hydrogen gas flow at the anode side produces water condensation and channel flooding for the serpentine-parallel flow-field topology. The work of Yamauchi *et al*. [46] shows that the flooding/plugging phenomena in the anode gas channel occur at low humidity when water is transported from the cathode to the anode through the membrane.

Transparent fuel cells provide useful information on water droplet formation, growth and movement, however, the direct visualization technique only provides qualitative data because of limited depth perception from the top of the transparent window, and also because of the highly reflective nature of GDLs, which make it almost impossible to quantitatively evaluate the volume of water [21].

4.2. Nuclear Magnetic Resonance (NMR) Imaging

Nuclear magnetic resonance (NMR) imaging, otherwise known as magnetic resonance imaging (MRI) is widely available, inherently three-dimensional, and capable of visualizing water in opaque structures. In recognition of these attributes, NMR has been successfully exploited for measuring the liquid water distribution of an operating fuel cell in situ, where liquid can be detected under the gas channel and land areas, in contrast to direct optical photography.

Perrin *et al*. [65] investigated the dynamic behavior of water within two types of ionomer membranes, Nafion and sulfonated polyimide, by field-cycling nuclear magnetic relaxation. Strong dispersions characteristic of better wetting have been observed in the case of polyimides than Nafion. By employing the MRI technique, Minard *et al*. [74] observed the formation of a dehydration front that propagated slowly over the surface of the fuel cell membrane—starting from gas inlets and progressing toward gas outlets of a PEMFC during 11.4 h of continuous operation with a constant load. Tsushima and Teranishi analyzed water transport in PEMFCs [75] as well as water content and distribution in a polymer electrolyte membrane [76-79]. Similarly, Zhang *et al*. [66] reported a direct water content measurement across the Nafion membrane in an operational PEMFC, employing double half *k*-space

spin echo single point imaging techniques. Feindel and co-workers [70-73] performed systematic *in-situ* investigations of in-plane water distributions and accumulation in the PEM. For example, ^{1}H NMR microscopy was employed to investigate the influence of co- versus counter-flow gas configurations on the in-plane distribution of water in PEM of the operating PEMFC. The co-flow configurations resulted in dehydration of the PEM at the inlets, while the counter-flow configurations effected a more uniform distribution of H_2O-(pem). Also, at the onset of H_2O (l) accumulation in the cathode flow field, the power output of the cell peaks, while further build up of water results in a decline in power output [72].

Although NMR imaging has provided valuable information about the water content in gas channels and membranes, it cannot be used to assess water content in the GDL due to the rapid attenuation of the signal in the carbon layer [70]. Therefore, NMR can only be used to see water in the membrane rather than within paramagnetic materials like carbon. Some other drawbacks along with NMR technique such as the limited temporal resolution, limited in-plane spatial resolution [79] and limited size of the magnet-core for fuel cell housing restrict its further application [117].

4.3. Beam Interrogation

4.3.1. Neutron imaging

The idea of using the neutron imaging technique for a PEMFC is based on the sensitive response of neutrons to hydrogen-containing compounds such as water [105], and insensitivity to common fuel cell materials [71]. It has been recognized as the only diagnostic tool that provides all of the three requirements for diagnostic tools in water management: *in situ* applicability, minimal invasiveness and the ability to provide local information [10]. The neutron imaging technique was first used in a PEM fuel cell to measure the water profile across the membrane in 1996 by Mosdale *et al*. [106]. In 1999, Bellows *et al*. [94] demonstrated the ability to determine water distribution in the membrane. The similar work was performed by Xu *et al*. [119], subsequently. In 2004, Satija *et al*. [105] employed in-plane neutron imaging of an operating PEM fuel cell and produced a time series of images to evaluate the water management of a fuel cell system.

Since then, a large number institutes equipped with neutron sources have explored this technique as an experimental tool to perform in situ non-destructive analysis on an operational PEM fuel cell, such as visualization of water accumulation along the in-plane direction to observe a two-dimensional distribution of water [92,99,102,120-122], especially the liquid water distribution in the cathodic flow fields and GDL [81,84,90,91,97,98,100-102], and the water accumulation [82,83,95-98] as well as content [80,85,88,90] in the channels of the cathode and anode.

Despite the various advantages mentioned earlier, the neutron imaging technique has limited application due to high costs and the rare availability of radioactive radiation equipment that provides neutron sources. Therefore, up to now, these researches are mainly concentrated amongst a few groups worldwide such as the Laboratoire Léon Brillouin at the Orphée Nuclear Reactor in Saclay, France [106], National Institute of Standards and Technology's Center for Neutron Research (NIST CNR) [86,88–99,105], the Penn State Breazeale Nuclear Reactor [96,98,101,102], the Paus Scherrer Institut (PSI) [97,103,104], and recently the Neutron Radiography Facility (NRF) at Hanaro, within the Korea Atomic Energy Research Institute (KAERI) [87].

4.3.2. Electron microscopy

Vapor condensation and liquid water morphology and breakthrough in porous layers of PEMFC can be observed by environmental scanning electron microscope (ESEM) [108,109,123]. Kaviany and Nam *et al*. [108,109] confirmed the presence of large droplets and high liquid saturation at interface of the CL and GDL due to jump in pore size. Besides, a model for morphology of liquid phase across multiple porous layers shows that the liquid morphologies deteriorate the efficiency of electrochemical reactions in CL and increase the water saturation in GDL. Finally, inserting a microporous layer (MPL) between CL and GDL can reduce both the droplet size and liquid saturation and improves the cell performance, as shown in Figure 7.

Figure 7. ESEM micrographs showing vapor condensation and liquid water breakthrough from (a) CL, (b) MPL, and (c) GDL. For each, micrographs at three different elapsed times are shown [108].
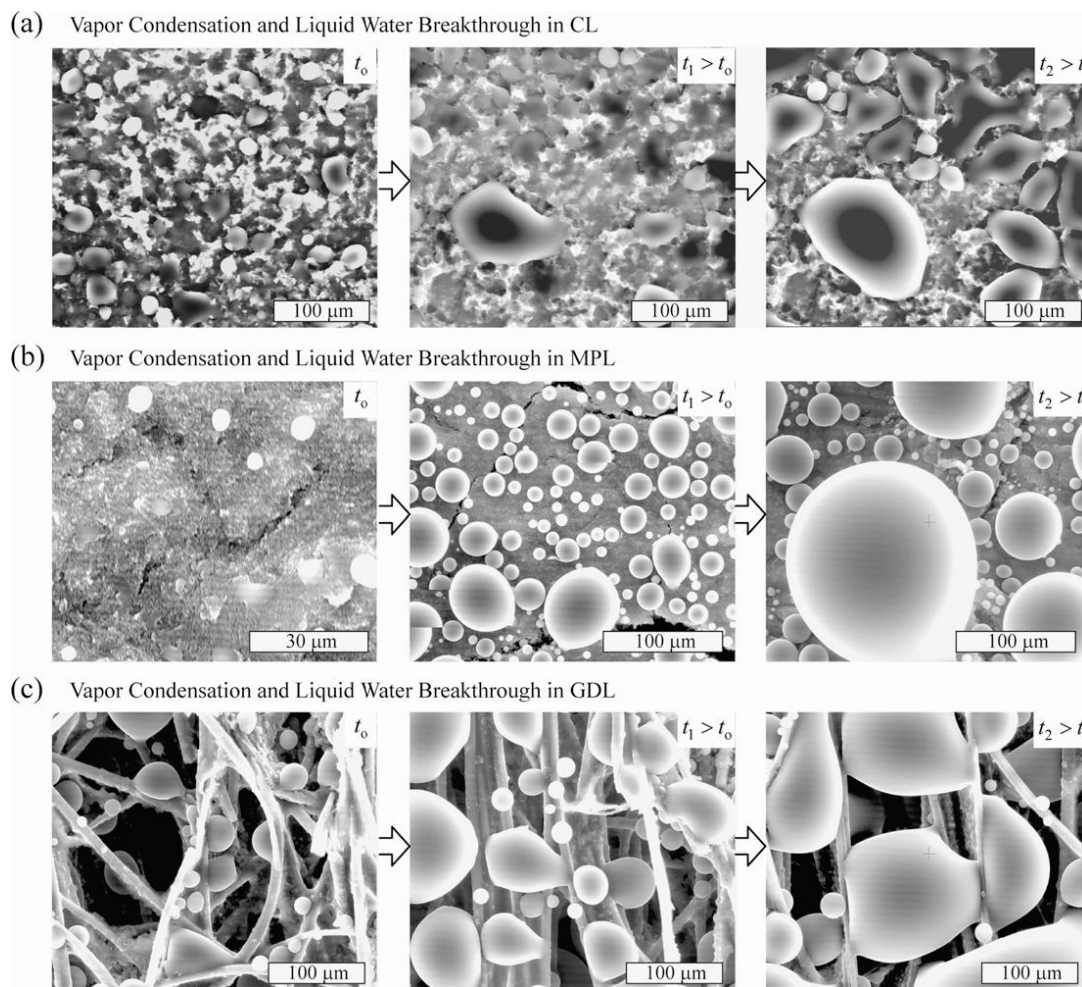
Besides, Yu *et al*. [107] adopted high-sensitivity double parallel conductance probes flow regime inspecting technique to inspect the flow regime of the gas-liquid two-phase flow in the PEM fuel cell and found that with the increase of the liquid superficial velocity, the frequencies of liquid slug and wave of liquid film increase.

4.3.3. X-rays

The X-ray image technique can give the temporal and spatial resolution, especially the use of synchrotron radiation makes it capable to reach higher spatial resolutions (the few microns of the X-ray beam cross-sections) coupled with high signal to noise ratios [124]. Therefore, this technique has strong potential for the visualization of water inside a PEMFC. Albertini *et al.* [124] reported the first experimental determination of a dehydration process occurring in the polymeric membrane of a fuel cell, observed in real time by *in situ* X-ray diffraction (XRD) of a very high-energy synchrotron radiation and the real-time changes of the water content based on the energy dispersive X-ray diffraction [111]. In addition, the liquid water saturation distributions [113-115] and accumulation [112,116] have been measured by X-ray microtomography [112,113] and synchrotron X-ray radiography [114-116]. However, the combination high temporal and spatial resolution to capture the rapid evolution of liquid droplets within the GDL is the challenge that X-ray microtomography technique has to face.

4.4. Fluorescence Microscopy

Fluorescence microscopy in conjunction with optical photography provides a method to visualize the micro-scale transport of liquid water in the surface of the GDL [57,118] and the dynamic water droplet behavior emerging from the GDL into a flow field [61]. However, due to the opaque nature of the GDL, this method has not been employed to elucidate the through-plane transport of the GDL to a great extent. Besides, the applicability of this method for *in situ* investigations is not yet unambiguous [117].

5. Modeling Works and Experimental Measurements on Water Management

5.1. Modeling Works

Numerous studies have devoted to developing theoretical models to describe the water management and liquid water transport in PEMFCs over the last decade, numbering dozens per year. Herein, four aspects of water management models are selected for further comment.

5.1.1. Dynamics models in water transport and distribution

Computational fluid dynamics (CFD) is gaining more interest as a tool to study water saturation, transport and distribution in PEMFCs, which will help in gaining an understanding of the mechanisms inside the fuel cell, aid in data analysis, and identify limiting parameters [125,126]. For example, Um and Wang [38] developed a unified water transport (diffusion, convection and electro-osmotic drag) model within the single-domain CFCD (computational fuel cell dynamics) framework with the aid of the equilibrium water uptake curve in the membrane phase to apply to elucidate water management in three-dimensional fuel cells with dry-to-low humidified inlet gases after its validation against available experimental data for dry oxidant and fuel streams. Shan and Choe [127] proposed a new model constructed upon the layers of a cell, taking into account the following factors: (1) dynamics in temperature gradient across the fuel cell; (2) dynamics in water concentration redistribution in the membrane; (3) dynamics in proton concentration in the cathode catalyst layer; (4) dynamics in reactant

concentration redistribution in the cathode GDL. Haddad *et al*. [128] developed a dynamical model considering the influence of gas consumption and humidification rates on water diffusion and membrane humidity. With the aid of the dynamical model, an appropriate control of the water content can be built to improving the electrical efficiency and minimizing power losses.

So far most of the theoretical models have concentrated on analyses under steady-state conditions. However, the transient transport behaviors in a PEMFC are more important, especially in applications. Serincan and Yesilyurt [129] developed a two-dimensional transient single-phase CFD model, incorporating water transport in the membrane and the flow and transport of species in porous gas diffusion electrodes to study the effect of step changes in cell voltage, cathode air pressure, and relative humidity during start-ups and failures of auxiliary components, such as the loss of pressure in the case of compressor or manifold malfunctions and the loss of humidity in the case of a humidifier malfunction. Le and Zhou [130] reported a general model specially focused on the liquid water management. The developed three-dimensional unsteady model with detailed thermo-electrochemistry, multi species and two-phase effects with the interface tracking by using the volume-of-fluid (VOF) method was implemented into the CFD software package FLUENT. Wang and Wang [131] developed a 3D transient model to study the transient dynamics of a PEMFC. They further performed numerical simulations for a single channel PEMFC undergoing a step increase in current density [31].

However, many CFD models have difficulties simulating PEMFCs with complex flow fields due to their heavy numerical computation load requirements. Currently published CFD models have mainly focused on the cases either in a straight flow channel or in a simple flow field [132].

5.1.2. Lumped models

Chen and Peng [132] developed a steady-state single cell lumped model consisting of 15 interconnected segments to describe distributions of liquid water accumulation, current density, and relative humidity (RH) in the flow channel of a PEMFC. Modeling results show that cathode inlet RH has significant influence on the uniformity of water content in the membrane and current density. Liquid water tends to accumulate in the GDL under the rib due to the suppression of gas flow in the channel. You and Liu [133] developed a two-phase flow and multi-component mathematical model with a complete set of governing equations valid in different components of a PEM fuel cell. For water transport through the membrane, the model includes the electro-osmotic drag, diffusion and hydraulic permeation. Chen *et al*. [134] proposed a five-layer theoretical model including anode and cathode GDLs, CLs, and the layer of PEM to investigate the steady and transient water transport phenomena by changing system parameters such as the RH of reactant gas, the porosity of GDL, and the membrane thickness. The results showed that if the humidification of the reactant gases is sufficient, the water management would be better for larger porosities of GDLs or a thinner membrane. Zhang *et al*. [135] built a model of water management systems which consist of stack voltage model, water balance equation in anode and cathode, and water transport process in membrane. This model can avoid fluctuation of water concentration in cathode and can extend the lifetime of PEM fuel cell stack. Ahmed *et al*. [136] developed a complete three-dimensional model including phase transformation to predict the water vapor and liquid water distributions and the overall performance of the cell for different current densities. The simulated results showed that the reactants and water distribution and

membrane conductivity in the cell depended on anode humidification and the related water management. The cathode channel/GDL interface experiences higher temperature and reduces the liquid water formation at the cathode channel. Indeed, at higher current densities the water accumulated in the shoulder area and exposed higher local current density than the channel area. Lum and McGuirk [137] used a steady-state, three-dimensional model of a complete PEMFC including both the anode and cathode to study the effect of electro-osmotic drag and diffusion of water across the membrane. The model shows that overall transport of water takes place from the anode to the cathode, therefore, it is crucial to humidify the anode reactants to keep the membrane well hydrated to prevent dehydration.

5.1.3. Flooding models

Shimpalee *et al.* [138] performed three-dimensional CFD simulations of a PEM fuel cell to investigate the effect of GDL flooding on fuel cell performance. The results show that increasing the degree of water flooding as it may occur in untreated GDL, reduces the effective diffusivity of gases dramatically, which in turn increases the concentration and surface over potentials and the fuel cell performance is decreased significantly. Baschuk and Li [139] developed a model with the effect of variable degree of water flooding in the cathode catalyst layer and cathode GDL on cell performance. Unfortunately, in their model phase change is neglected and the volume fraction of liquid water in the porous regions must be specified. Paquin and Fréchette [140] developed a simple one-dimensional model to analyze water management in air breathing small PEMFC. The results show that decreasing the ratio between thermal and mass transport resistance under a certain point leads to flooding problems while increasing this ratio leads to dry-out of the polymer electrolyte membrane in air breathing PEMFC. A three-dimensional model presented by Natarajan and Nguyen [141] considers the effects of flow rate, inlet humidity and temperature on the liquid water flooding in the cathode. The works of Meng and Wang [19,142] also predict water flooding inside a PEMFC and the liquid water effects in the cell performance. Wang affirmed that when the current density is beyond a certain value, too much water will be produced at the cathode and the gas will be saturated by water vapor, then the phase of water vapor begins to change into a liquid phase resulting in cathode flooding [38]. Furthermore, when the current density is greater than 1.4 A cm^{-2}, at the condition of RH 100% for both cathode and anode, water flooding will happen in the cathode, which will be in the case of severe flooding when the water activity (p_w/ p_w^{sat}) is in excess of 3 [14]. Similarly, Shah *et al.* [143] also took account with the effect of water activity on the flooding and membrane hydration in a comprehensive non-isothermal, one-dimensional model of the cathode side of a PEMFC. Lin *et al.* [144] developed a two-phase, one-dimensional steady-state, isothermal model of a fuel cell region consisting of the catalyst and gas diffusion layers to investigate the effect of water flooding in the gas diffusion layer and catalyst layer of the cathode on the overall cell performance. The simulation results confirmed that the water-flooding situation in the catalyst layer is more severe than that in the backing layer since water is first produced in the catalyst layer. Wu *et al.* [145] developed a two-dimensional isothermal transient model and the transient results demonstrated that the dynamic behavior of fully humidified PEMFC is mainly determined by the cathode flooding conditions and oxygen transport in the GDL; the transient variations in the dry cathode case are well within 0.3 s, while this variation periods are prolonged to around 1 s if the cathode is severely flooded.

The above models have not taken the pore diameter distribution into consideration. Liu *et al.* [146] studied membrane hydration and electrode flooding by developing a 2D partial flooding model in which the pore size distributions are assigned for the hydrophobic and hydrophilic pores of the GDL. The liquid water produced is considered to condense in hydrophilic and hydrophobic pores in sequence if the water vapor pressure is greater than the capillary condensation pressure. In addition, a GDL including MPL with a linear porosity $0.4\,x + 0.4$ is the best favorable for liquid water draining from catalyst layer into the gas channel when the total thickness of the GDL and MPL is kept constant and the MPL is thinned to 3 μm [147]. Recently, Karimi *et al.* [148] proposed a partially flooded GDL model to estimate the operating conditions under which water flooding could be initiated in a PEMFC stack. The model can predict the stack performance in terms of pressure, species concentrations, GDL flooding and quality distributions in the flow fields as well as the geometrical specifications of the PEM fuel cell stack.

5.1.4. Other water transport and water management models

Zamel and Li [149] developed a steady-sate isothermal model demonstrating that the catalyst layer is important in controlling the water concentration in the cell and the cross-flow phenomenon enhances the removal of liquid water from the cell. Moreover, a shoulder/channel width ratio of 1:2 is found to be an optimal ratio for water transport. Yan *et al.* [150] investigated numerically the coupling effects of mass diffusion and temperature gradient on the water distribution in the membrane, which is useful for selecting the optimal membrane material and estimating the gas-inlet temperature or working density in designing a PEMFC.

Karimi and Li [151] studied the electro-osmotic flow of water from anode to cathode by a model incorporating the electrokinetic effect and found that the electroosmotic drag coefficient increases with the pore diameter. Similarly, Falcão *et al.* [152] presented a steady-state one-dimensional model to study the combined effect of diffusion and electro-osmotic drag on the water transport through the membrane. The model can provide suitable operating ranges adequate to different applications (namely low humidity operation) for variable MEA structures.

Matamoros and Brüggemann [153] developed a non-isothermal and three-dimensional numerical model to determine the transport of water in the polymer membrane, phase change of water in the cathode porous medium and capillary flow to the gas channels. Results show that there may be severe mass transfer limitations depending either on the design or on the water management of the cell.

Wang *et al.* [154] used a two-phase channel model to simulate the flow of liquid water in mini-channels of a PEMFC. Moreover, they affirmed that capillary action is found to be the dominant mechanism for water transport inside the two-phase zone of the hydrophilic structure [155]. Zhu *et al.* [156] investigated the dynamic behavior of liquid water entering a PEMFC channel through a GDL pore by performing two-dimensional, transient simulations employing the VOF method. The simulation results show that the height of the channel as well as the width of the pore have significant impacts on the deformation and detachment of the water droplet, and the coalescence of two water droplets can accelerate the deformation rate and motion of the droplets in the microchannel. Further, they simulated the processes of water droplet emergence, growth, deformation and detachment by transient three-dimensional two-phase flow model and found that the wettability of the microchannel

surface has a major impact on the dynamics of the water droplet, with a droplet splitting more readily and convecting rapidly on a hydrophobic surface, while for a hydrophilic surface there is a tendency for spreading and film flow formation [157]. Similarly, Chen *et al.* [158] also found that droplet removal can be enhanced by increasing flow channel length or mean gas flow velocity, decreasing channel height or contact angle hysteresis, or making the GDL/gas flow channel interface more hydrophobic. Golpaygan and Ashgriz [159] computationally studied the mobility of a water droplet in a channel of a PEM fuel cell and found that the surface tension is the most important effect factor. He *et al.* [160] developed a 2-D, two-phase, multicomponent transport model and confirmed that the transport of liquid water through the porous electrode of a PEMFC employing an interdigitated gas distributor is driven by the shear force of gas flow and capillary force.

Besides, some mathematical models were developed to evaluate the humidification effect on PEMFC performance [161-164]. For example, Ahmed and Sung employed three-dimensional, non-isothermal models to investigate the effect of humidification [165], GDL permeability [166], channel geometrical configuration and shoulder width [167] on water management, and predict the distributions of water vapor and liquid water and the related water management for systems operating at different current densities [168].

Of course, the PEMFC models are not only limited to the above. More detail models can be referenced in a comprehensive review of fundamental models for PEMFC engineering provided by Wang [22] and transport models reviewed recently by Weber [37] and Siegel [169].

5.2. Experimental Measurements

5.2.1. Water transport and distribution

Quick *et al.* [170] developed a new *ex situ* test method to investigate the water transport in gas diffusion media for PEMFCs, and the research was focused on properties of GDLs. The experimental results show that water transport rates depend not only on the GDL properties, but increase exponentially with cell temperature. Colinart *et al.* [171] investigated water transport within PEMFC by systematic measurements of the water transport coefficient and found that the hydrogen flow rate, the amount of vapor injected at cathode inlet, and the temperature are the main parameters influencing the water transport coefficient. Wang *et al.* [172] investigated water formation and transport using a microfabricated experimental structure with distributed water injection as well as with heating and temperature sensing capabilities.

A technique based on the entrance region pressure drop measurements was presented for monitoring fluid flow mal-distribution in individual channels [173,174]. In these works, the instantaneous channel flow rate (flow mal-distribution), pressure drop, and the flow structure were studied by using the entrance region pressure drop method, differential pressure transducers, and high-speed visualization, respectively. A quantitative description of the channel flooding is established and the pressure drop signatures for each flow pattern are identified. The measurement results show that the two-phase flow at low superficial air velocities is dominated by slugs or semi-slugs, leading to severe flow mal-distribution and large fluctuations in the pressure drop. At high air velocities, a water film is formed on the channel walls if they are hydrophilic.

Murahashi *et al*. [175] investigated water transport through the membrane of a PEMFC by measurement of the net drag under various feed gas humidity conditions and found that there is a certain resistance related to water transport at the cathode membrane interface in association with water production. Stumper *et al*. [10] developed a diagnostic tool that combined membrane resistance and electrode diffusivity (MRED) measurements with current mapping [176] to detect the distribution of water in the membrane across the active area, and the total amount of liquid water present in the anode or cathode chamber could be determined.

Capillary pressure plays important role in water transport and removal. A micro-fluidic device was designed to measure the capillary pressure as a function of liquid water saturation in PEMFC gas diffusion layer with complex, heterogeneous wetting properties [177]. The measurements discovered a hysteresis between the liquid intrusion and gas intrusion curves, *i.e.*, gas diffusion media appear hydrophobic during most of the liquid intrusion curve and hydrophilic during most of the gas intrusion curve. The capillary pressure curves were measured [178] for both the total pore network and the pore network consisting of only hydrophilic pores. This enables the determination of capillary pressure curves directly relevant to the study of gas diffusion layer flooding. It was confirmed that the capillary pressure is positive during water injection and negative during water withdrawal [179].

5.2.2. Diagnosis of water flooding and membrane drying

Several methods for detection of water flooding and membrane drying have been established by testing cell impedance response in conjunction with cell voltage or pressure drop as well as current distribution [2,17,50]. For example, Fouquet *et al*. [180] monitored flooding and drying out of a PEM fuel cell using a model-based approach coupled with ac impedance measurements. They found that a cell flooding occurs in two steps: first, accumulation of liquid water inside the GDL while cell voltage drops quite slowly and, after several minutes, the droplets aggregate and block the gas channels, impeding reactants diffusion to the catalyst sites and inducing in turn a rapid cell voltage drop as shown in Figure 8. Figure 8 also confirms that flooded and dry conditions can lead to the same voltage drop. Dai *et al*. [181] reported a simple method to measure the water transport rate across the GDL. Based on the measurement results, the fuel cell operating conditions, such as current density, temperature, air stoichiometry and relative humidity, corresponding to membrane drying and flooding conditions were identified for the particular GDL used. This method can help researchers develop GDLs for a particular fuel cell design with specific operating conditions and optimize the operation conditions for the given PEM fuel cell components.

The pressure drop between the inlet and outlet channels can be used as a diagnostic signal to monitor the liquid water content in the porous electrodes, because of the strong dependence of the gas permeability of the porous electrodes on liquid water saturation, which corresponds to the extent of flooding [182]. It can be used with no modification to existing fuel-cell assembly to give real-time flooding information in the electrode backing layers during operation. He *et al*. [24] employed an electrode flooding monitoring device to investigate the correlation between the fuel-cell performance and the liquid water saturation level in the backing layers, the effects of various operating parameters, and the dynamics and hysteresis behavior of liquid water in the backing layers. The results confirmed that the hysteresis behavior of fuel-cell performance during water imbibition and drainage cycle is

attributed to the difference in water-removal rate by capillary force and the difference in membrane conductivity.

> **Figure 8.** (A) Flooding of a fuel cell at constant pressure, temperature and stoichiometries, with fully humidified reactants and a slowly increasing current. (B) Mean cell voltage of a fuel cell in flooded, normal and dry condition, as a function of time and relative humidity of inlet gases, with constant pressure, temperature, stoichiometries and current are shown [180].
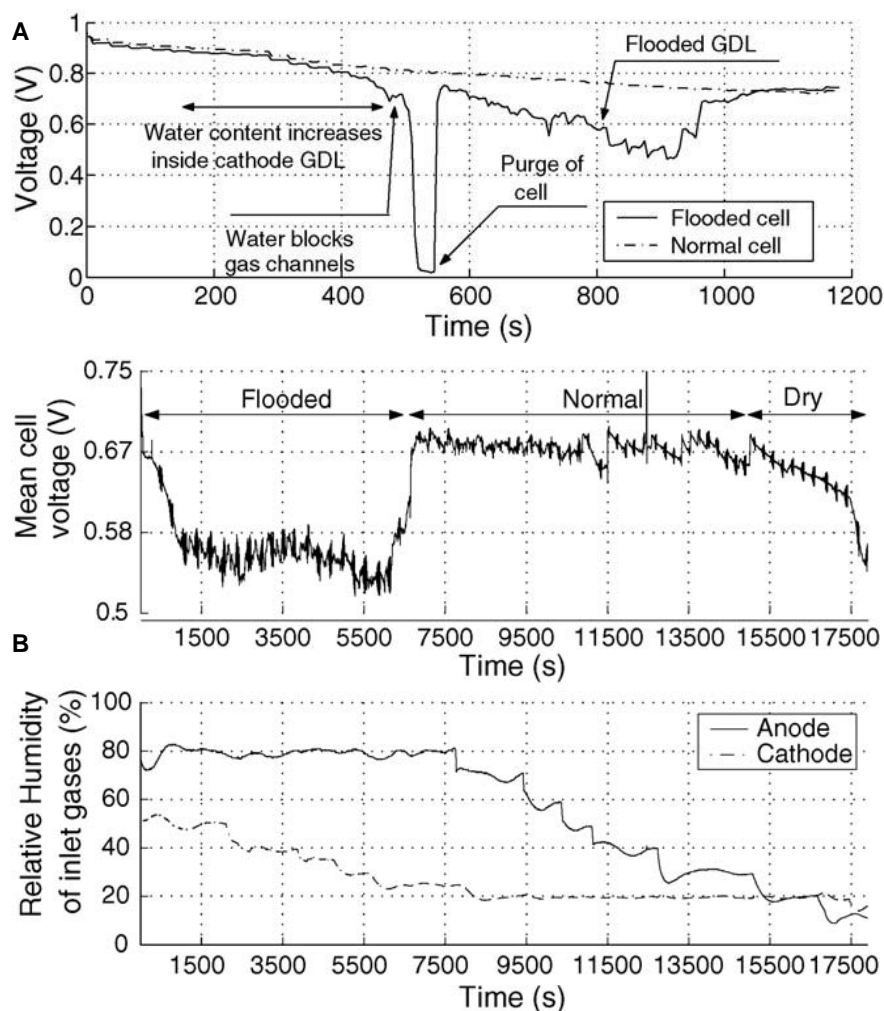
Yoon *et al.* [183] measured current distribution in a single cell by using a specially designed single cell which was composed of 81 compartments and suggested that the flooding process begins at the gas outlet region of a cell, then, it propagates to the inlet area. The drying process of a cell seems to occur in the direction opposite to the flooding case. Hottinen *et al.* [184] studied the effect of cathode structure on the performance of planar free-breathing fuel cell. They found that very high power densities for free-breathing fuel cell were achieved with thin gas diffusion backing, however, the cell was also vulnerable for flooding, especially in the horizontal direction caused a significant increase in mass diffusion overpotential and also increased the cell voltage fluctuation in short time-scale.

Santarelli and Torchio [185] characterized the behavior of a single PEMFC with variation of the values of six operation variables: cell temperature; anode flow temperature under saturation and dry

conditions; cathode flow temperature under saturation and dry conditions; and reactant pressure. The experimental results demonstrated that excessive humidification or lower cell operation temperature could cause electrode flooding especially at high current density values on the cathode side, when, oxygen diffusion is the limiting step [186]. The transport phenomena related to fluid flow through PEMFCs with microchannels has been studied by electrochemical impedance technique. The results show that in smaller channels mass transportation resistance increase due to flooding, but that this effect may be offset by a reduction in dead zone area [187].

Natarajan and Nguyen [18] used a segmented electrode/current collector setup to examine the effect of oxygen flow rate, anode sparger temperature, and hydrogen starvation on the spatial and temporal distribution of local current densities along a single gas channel in a PEM fuel cell. They found that when water removal rate was not sufficient electrode flooding occurred in segments that were farthest from the gas inlet. Once the liquid water fills up the majority of the pores in an electrode, the continuity of the gas phase within the electrode is severely compromised and the sustainable current density will be in the order of a few tens of milliamperes/cm^2 as the limiting currents observed in their experiments.

Kimball *et al.* [188] examined the process of flooding with a single-channel fuel cell that permits direct observation of liquid water motion. As product water flows through the largest pores in the hydrophobic GDL, drops detach from the surface, aggregate, and form slugs. Flooding in PEMFCs occurs when liquid water slugs accumulate in the gas flow channel, inhibiting reactant transport. They affirmed that flooding is not the result of capillary condensation in the GDL, but rather liquid blocking oxygen transport across the gas/GDL interface.

Besides, in order to investigate the flooding of PEMFC stack, Buaud *et al.* [189] developed a water balance calculation comparing the amount of water produced by the electrochemical reaction to the amount of water transported as vapor in the exit air flow minus the amount of water incoming the stack in the ambient air by constructing a nondimensional number called the Flooding Number relevant to stack flooding.

6. Water Management Strategies

Proper water management is vital to guarantee achieving maximum performance and durability of PEMFCs. Therefore, how to maintain the delicate balance between membrane hydration and avoiding cathode flooding has become the principal goal to develop strategies for proper water management. The main water management strategies developed so far may be summarized as follows.

6.1. Optimum Operational Conditions

PEM fuel cell operating conditions include inlet humidity of the feed streams, cell temperature, operating current density, back pressure, air and fuel stoichiometric flows, and so on. Extensive experimental procedures can be used to quantify these factors, which can be classified in different types: intrusive, non-intrusive, *in situ* and *ex situ* methods. Among these methods, *in situ* methods can test the individual cell or the stack performance during its operation, while, *ex situ* methods cannot be used during fuel cell operation. In addition, the intrusive methods usually use sensors in the cell to modify the fuel cell state (segmentation of the electrodes, for example), however, the methods can only be implemented in a specific kind of fuel cell design, while the non-intrusive methods can be implemented

in all fuel cells, and do not use inner sensors [26]. Some non-intrusive *in situ* methods, such as polarization curve (I-V curve), electrochemical impedance spectroscopy (EIS), membrane resistance measurement and pressure drop measurement, are reproducible on a large set of fuel cell designs and that can deliver an optimum set of information about the evolution of many parameters during fuel cell operation. Such methods are ideal to be used as fuel cell testing protocols.

Manipulation of the operational conditions such as reactant humidity and flow rate, operating temperature and pressure, is a very common and efficient water management strategy. For example, increasing the humidity level of inlet gas at the anode will lead to an increase in current distribution heterogeneities owing to the decrease of the amount of liquid water transferred from the cathode to the anode by back-diffusion [18]. Increasing reactant flow rate especial cathode reactant can improve the cell performance due to the higher stoichiometry and the flush of the water out of the cell system through evaporation and advection [14,49,50,190,191]. A recovery of the flooded cell was observed after applying a quick cell temperature step from 40 to 50 ℃ while fixing the other parameters (air flow rate, cell voltage) [24]. Besides, cell performances can be improved by setting a pressure gradient between the cathode and the anode ($P_a < P_c$) to force liquid water through the membrane from cathode to anode side. This strategy is called "anode water removal" [192]. However, this class of strategies often causes significant parasitic losses that are directly linked to pressure, volume flow rate and pressure drop, as well as the possibility of membrane rupture in designs that do not adequately support the MEA [27].

6.2. Cell System Design

6.2.1. Gas humidification system

As discussed above, a critical requirement of PEMFCs is to maintain a high water content in the electrolyte to ensure a high ionic conductivity. The ionic conductivity of the electrolyte can be maintained high when the membrane is fully humidified, and offers a low resistance to current flow and so increases the overall efficiency of PEMFCs. Various humidification designs such as internal humidification, external humidification, and direct injection methods are used in the PEMFC to maintain hydration level of the polymer membrane.

Internal humidification is based on the principle that the electrolyte absorbs and retains water under the operating conditions, which is also called "self-humidification" [34]. However, this humidity control is difficult and is not appropriate for large systems such as in automotive applications. Furthermore, steady-state multiplicity might occur [193]. Gas is passed through a water column of a humidifier bottle in the external humidification method. The humidifier bottle temperature controlled independently from cell fixture temperature to get the desired gas temperature and relative humidity. The external humidification method is widely used in small scale laboratory fuel cell experiments due to its simplicity, but needs an additional humidification apparatus [194]. However, it should be noted that running a fuel cell with bubbler humidifiers is not trivial taking into account that every single screw or plate should be thermally insulated to avoid condensation, and maintaining exact inlet conditions or measuring exact dew points before entering the cell is very difficult.

Steam injection is a widely used method for air conditioning, but it is not economic for automobiles as it needs much energy to generate steam. An additional amount of liquid water is injected directly into the fuel cell in the liquid injection design. Nguyen *et al*. [195] found that the direct liquid water injection used in conjunction with the interdigitated flow fields as a humidification technique is an extremely effective method of water management. This method is compact, easily controllable and moreover does not need much energy for humidification. The downside of the direct water injection is the possibility of flooding in the fuel cell.

For commercialization of fuel cells, humidifiers must meet both high humidification performance and low energy consumption for humidification. However, it is difficult to meet all of these requirements simultaneously. As each humidification method has its own advantages and disadvantages, an ideal gas humidifying method for automotive applications could be a hybrid form of the above mentioned methods. Kim *et al*. [196] developed a sub-scale gas humidifier consisting of an injector, an enthalpy mixer and a water-retrieval unit, where, water injection into the enthalpy mixer is chosen instead of direct injection into the fuel cell to enhance the performance of humidification and prevent water flooding or clogging in the gas channels of the fuel cell.
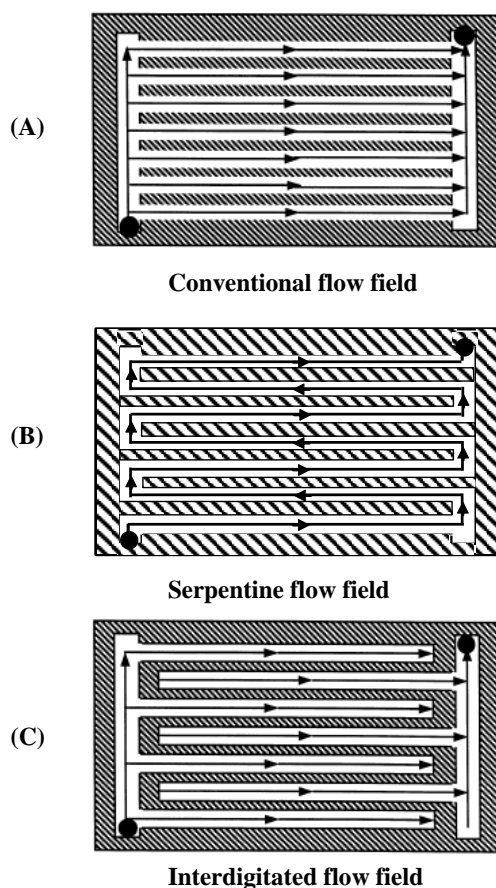
6.2.2. Flow field design

An appropriate flow channels design plays a major role in the water management problems, because the water transported from the GDL must be removed out of the cell system via these flow channels, which has been considered to be the most successful strategy for dealing with water flooding issues [121,197]. Up to now, three typical flow fields, *i.e.*, the conventional flow field, the serpentine flow field and the interdigitated flow field, are mainly adopted in the practical application as show in Figure 9.

In the conventional flow field, diffusion is the dominant mechanism for the transport of reactants and products, which limits the transport rate of reactants leading to the excessive accumulation of liquid water and final water flooding [15,198,199].

For serpentine flow channels [200,201], the reactant gas experiences a pressure drop and concentration change along the channel; since the channel cross-section is small, in the order of 1 mm × 1 mm or smaller, while the channel length is very long, in the order of meters, the pressure drop at the corresponding location between the adjacent channels becomes substantial, significant pressure gradient is thus set up across the porous electrode, much larger than the pressure gradient along the channel direction, resulting in considerable cross leakage flow between the adjacent channels. This significant cross leakage flow through the porous electrode induces a strong convection in the electrode, bringing the reactant gas to the catalyst layer for electrochemical reaction and removing the product water from the reaction sites and electrodes. Therefore, this flow field design with a convective feature is the most widely used and has achieved the "industrial standard" level, since under the same operating and design conditions PEM fuel cells with serpentine flow channels tend to have the best performance and durability/reliability. However, serpentine flow channel layout is not the ideal flow field configuration, and has a number of problems. First, it typically results in a relatively long reactant flow path, hence a substantial pressure drop, consequently significant parasitic power loss associated with the cathode air supply. Second, a significant decrease of reactant concentration occurs from the

flow channel inlet to the outlet, leading to considerable Nernst losses for practical cells of large sizes. Most important of all, the use of serpentine flow channel layout often causes the membrane dehydration near the channel inlet region and liquid water flooding near the channel exit. These issues have caused the often-observed phenomenon of achieving good performance for small cells, and poor performance for apparently the same cells with large sizes, and are primarily responsible for the difficulty in establishing scaling laws for PEM fuel cells [121].

Figure 9. Three typical flow field designs (A) conventional flow field, (B) serpentine flow field and (C) interdigitated flow field are shown [195].

Conventional flow field

Serpentine flow field

Interdigitated flow field

In the interdigitated flow field, the flow channel design is a dead-end mode, forcing the gas to flow through the porous GDL and converting the reactants transport from a diffusion mechanism to a forced convection mechanism. The shear force resulted from the gas flow helps flushing any liquid water out of the electrode, thus effectively reducing the water flooding and significantly improving the cell performance [195]. But, similar to the serpentine flow field, the needed higher pressure forcing gas to flow through the GDL can lead to significant additional power less and membrane drying at low current densities.

In order to overcome the drawbacks of the above flow field design, Li *et al.* [121] developed a design procedure for flow channels in PEM fuel cells. The main design philosophy is based on the determination of an appropriate pressure drop along the flow channel so that all the liquid water in the cell is evaporated and removed from or carried out of the cell by the gas stream in the flow channel. On

the other hand, the gas stream in the flow channel is maintained fully saturated in order to prevent membrane electrolyte dehydration. Experimental results demonstrated that for the present flow channel design water flooding phenomenon is effectively prevented. Recently, a convection-enhanced serpentine flow field was developed by modifying the patterns of conventional serpentine channels to enhance the water removal and mass transfer [202].

Besides the above three flow field designs, there are some novel designs. For example, a baffle-blocked flow field was designed to force more fuel gas in the flow channel enter the GDL and CL to enhance the chemical reactions and then the performance of the PEMFC systems [203]. A triangular microchannel flow field was developed, in which, water droplets are lifted into a secondary channel, and removed from the fuel cell by capillary action. The new flow field design stabilized the cell at 95% of its initial performance compared to 60% when using the standard design [204]. A stepped flow field was proposed to improve the reactant concentration distribution, local current density distribution, water vapor concentration distribution and cell performance [205].

In addition, UTC Fuel Cells used a water-exchange scheme and the key to this water management system is the water transport plate (WTP), a porous bipolar plate in which the pores are filled with liquid water. The WTP is gas impermeable, similar to a regular bipolar plate, preventing gas ingestion to the coolant streams while allowing water exchange. The reactant gas streams are maintained at a higher pressure than the pressure in the coolant stream with a predetermined pressure difference between the gas and the coolant flow fields. This pressure difference causes excess liquid water in contact with the WTP to be wicked into the WTP and moved to the coolant passage network at a local level. Thus, issues associated with liquid water accumulation along the channel are eliminated [206].

Moreover, incorporation of special hydrophilic wicking structures into cathode flow channels can redistribute liquid water and accelerate water removal [29,207,208]. For example, a cathode serpentine flow field mounted with one or two strips of absorbent wicking material (such as PVA sponge, cotton cloth, cotton paper, etc.) was used, achieving improved water removal at a current density of 1.2 A cm^{-2} [208].

In summary, an ideal flow channel design should provide a uniform concentration of reactants and a reasonably small pressure drop between the inlet and outlet of the channel to minimize the parasitic losses, a mechanism to maintain membrane enough hydration over the entire cell avoiding membrane dehydration near the channel inlet; synchronously, a mechanism for the effective removal of liquid water to prevent water flooding of the cell near the flow channel outlet [121].

6.2.3. Other optimum cell system design

As an efficient water management strategy, the electroosmotic (EO) pumping technique has been examined to mitigate cathode channel flooding by the Santiago group [209-211]. The operating principle is that water formed from oxygen reduction reaction at the cathode is forced out of the GDL via hydrophobic forces where it coalesces into droplets. Liquid water droplets are wicked into the hydrophilic porous glass structure of the EO pump. Once the EO pump structure is adequately saturated with water, EO pumping actively drives water through the porous glass structure and into integrated water reservoirs in the acrylic top plate. Their research results show that under certain operating conditions, removing water from the cathode using integrated EO pumping structures

improves fuel cell performance and stability [209]. Later, Santiago *et al.* [210] presented a detailed study of an active water management system using a hydrophilic, porous cathode flow field, and an EO pump for water removal, and revealed the mechanisms and dynamics associated with EO pump based recovery from catastrophic flooding. Furthermore, the EO pump requires less than 1% of the fuel cell power to recover from near-catastrophic flooding, prevent flooding, and extend the current density operation range.

Besides, Hogarth and Benziger [212] demonstrated an auto-humidified operation of a channel-less, self-draining fuel cell based on a stirred tank reactor. The new design offers substantial benefits for simplicity of operation and control including: the ability to self-drain reducing flooding, the ability to uniformly disperse water removing current gradients and the ability to operate on dry feeds eliminating the need for humidifiers.

6.3. MEA Material and Structure Design

The above system design strategies often add auxiliary systems to the basic fuel cell system and hence significant complexity and additional costs. A simpler strategy for water management through MEA material and structure design is preferred, due to the absence of associated parasitic load [213]. This strategy involves optimization and innovative design of the MEA material properties and structures.

6.3.1. Electrolyte membrane material design

Thinner membranes (*ca.* 10 μm) have demonstrated better water management characteristics due to the shorting of the distance of the water back-diffusion process, synchronously, reducing the need for anode humidification and lower ohmic losses through the membrane as well as being much less sensitive to temperature and current density changes. However, thinner membranes are often associated with poorer durability and higher gas crossover rates, which has limited the practical membrane thickness to about 25–40 μm for fuel cell applications [214]. Watanabe *et al.* [215,216] propose self-humidifying polymer membranes with porous wicks, Pt particles and hygroscopic particles to mitigating the issue of cathode flooding under the condition of minimal to zero air-side external humidification.

Besides, in order to simplify water management, developing alternative membranes operational at higher temperatures than 100 ℃ has attracted extensive interest because above the boiling point of water, the operation of PEMFCs only involves a single phase of water, *i.e.*, water vapor, and therefore can be simplified. These strategies involve organic-inorganic hybrid membranes containing functionalized silica [217-219], metal oxide-Nafion composite membranes [220], self-conducting benzimidazole oligomers [221], *etc*. These high temperature polymer electrolyte membranes for operation above 100 ℃ have been reviewed by Li *et al.* [222]. However, the mechanical properties and durability of these high temperature membranes need to further verify and optimize.

6.3.2. GDL material and structure design

Among the PEMFC components, the GDL plays a crucial role because the GDL has lots of important tasks in the fuel cell. On the one hand the reactant gases have to be distributed

homogeneously from the flow field to the CL through GDL for the electrochemical reaction. On the other hand the GDL should remove heat and excess water from the electrode to prevent local hotspots and catalyst flooding. The required properties of a GDL are therefore good electrical and thermal conductivity as well as high thermal and chemical resistance and enhanced water and gas permeability. However, some of these requirements are contradictory. For example, air and water permeability increase with higher porosity, contrary to mechanical properties, electrical and thermal conductivity. Additionally all these mentioned characteristics are influenced by the GDL thickness, hydrophobicity and alignment of the carbon fibers. In general, there are three main types of carbon fiber substrates which are employed as a GDL: carbon paper [223,224], carbon cloth [225] and carbon non-woven [226]. Ralph *et al*. showed that the carbon cloth performs better than the carbon paper under fully humidified conditions due to an efficient water removal [227]. On the contrary, carbon paper provides higher fuel cell performance under dry operating conditions, probably due to better water retention behavior [170]. In addition, using carbon fiber as GDL material, water is inclined to emerge over the surface of the flow channels in the form of droplets, while water tends to move along the sidewall of the channels in the form of films and slugs with carbon cloth and carbon slugs, respectively. Advani *et al*. believed that the water droplet removal mechanism was far more effective than the film and slug removal mechanism [21].

The GDL plays a crucial role in water management that maintains the delicate balance between membrane hydration and water flooding. To avoid flooding the porous interstitial spaces with accumulated water, gas diffusion media are commonly treated with a hydrophobic agent such as PTFE to change its wetting characteristics so that the water is better expelled. Thus, most of the water, especially the product water at the cathode, can be efficiently removed from the CL through the GDL to the flow field channels. Such a treatment leads to a mixture of hydrophilic and hydrophobic pores in the GDL [178] and hence, inhibits water condensation in the GDL pores completely and ensures a low water saturation level [228]. Hence, the hydrophobic pores allow a pathway for gas transport whereas the hydrophilic pores facilitate liquid water transport [224,229]. The effect of PTFE content on PEMFC performance has been extensively studied in many studies [110,223,224,228,230]. Increasing the PTFE loading leads to higher hydrophobicity, but lowers the electrical conductivity at the same time [223]. Additionally, the reduced porosity of GDL will result in higher mass transport resistance [223,226,231]. However, insufficient water removal capability occurs at too low PTFE content. Therefore, optimum PTFE content should be in the range of 10%−30% [110,228,230,232-234]. Unusually, Tüber's investigation [49] suggested that the hydrophilic GDL turned out to be the more effective media in reducing water flooding, due to effective water removal from the CL to the GDL in small fuel cells for portable applications operated at ambient pressure and low temperatures (<30 °C) and in the current density range of less than 0.25 A cm^{-2}. Meanwhile, the increased PTFE content in the GDL hampered the ejection of water from the catalyst layer to the flow channels through the GDL, especially at conditions with high relative humidity. This would result in water flooding of the catalyst layer. Moreover, the capillary force in the GDL was not the main driving force for water transportation, instead, the shear force of fluid and water evaporation were the dominant driving forces due to the relatively larger pores of the GDL compared to those of the CL and MPL [228].

On the other hand, Kong *et al*. [235] verified that the pore-size distribution is a more important structural parameter in affecting the cell performance characteristics than the total porosity. They assumed that water transport occur simultaneously in two ways: micro- and macro-transport. The role of micropores is in transferring the condensed water from the condensation sites towards the flowing macro-droplets of water. Macropores (5–20 μm) contribute to reducing the mass transport limitation due to water flooding since they can provide gas diffusion paths toward the catalytic region until the micropores and the smaller pores are completely closed by water droplets. However, if the macropore volume is too large, the electric conductivity of the electrode is decreased. Chu *et al*. [236] reported that a higher porosity in the GDL would lead to a higher consumption of oxygen. However, a high porosity would be accompanied by water flooding in the GDL, which would markedly decrease the cell performance. Lee *et al*. studied the effect of fabrication method of GDL on the cell performance. The results show that in the rolling method, the distinctive drop in cell voltage suggests that the presence of water saturation in the diffusion layer not only imposes more resistance to gas diffusion toward the catalyst layer, it also influences catalyst flooding (partial coverage of catalyst particles with liquid water) where as, in the spraying and screen printing methods, lower diffusion losses were observed since better distribution of pores makes the liquid and gas phase separate effectively [237]. Liu *et al*. [146] found that in low voltage range for a smaller GDL average pore diameter, overpressure for the hydrophobic pores will be higher, and that the flooding is lighter, so higher current density is shown.

Besides, Wang *et al*. [238] proposed a new treatment of GDLs by sucrose carbonization in order to obtain high hydrophobicity with low PTFE loading. Jiao and Zhou [239] proposed three innovative GDLs with different micro-flow channels to solve liquid water flooding problems. Their opinions are that the conventional GDLs are not effective for water removal because the micro-structure and the size of the pores of conventional GDLs are very arbitrary, and the sizes of the pores are very small (10 and 30 μm). Due to the physical features of the conventional GDLs, water flooding frequently happens in the GDL and catalyst layer of practical PEM fuel cells. The main reason causing frequent flooding is that the arbitrary structure of conventional GDLs does not allow a well-organized liquid water flow. Recently, Zhang *et al*. [240] developed a metallic porous medium with improved thermal and electrical conductivities and controllable porosity based on micro/nano technology for its potential application in PEM fuel cells. The small thickness and straight-pore feature of this kind of gas diffusion medium, made of 12.5 μm thick copper foil, provides improved water management even at low flow rates.

6.3.3. MPL material and structure design

Adding a sub-layer micro porous layer (MPL) between the catalyst layer and the GDL is considered an effective method to improve liquid water drainage and gas diffusion, as well as minimize electronic contact resistance with the adjacent CL [7,21,109,229,231,241-253]. In MPL, consisting of a mixture of carbon black (CB) and a hydrophobic agent such as PTFE, the pore diameter is in the range of 0.02–0.5 μm [254] compared to that between 1μm and 100 μm in the GDL [229,255]. According to the assumption that water condensation occurs hardly in hydrophobic pores smaller than 1 μm, GDLs with an additional MPL have lower water saturation levels, leading to higher gas transport at the CL [231,243,256]. Qi *et al*. speculated that the microporosity and more uniform pore distribution might

be the major contributors to the improved water management, and the improved water management could make, not only the MPL itself, but also the catalyst layer less likely to be flooded [231].

Regarding the explanation of the role of MPL in water management, some studies have hypothesized that, depending on several characteristics like hydrophobicity, thickness, pore diameter and porosity, the MPL is able to block liquid water at the interface to the cathode CL and acts as a valve that forces water away from the cathode side through the membrane to the anode by increasing the back diffusion [231,244-246,254]. In contrast to the above claim, another explanation is that the MPL provides effective wicking of liquid water from the CL into GDL and finally to the flow field channels [109,110,243]. However, this effect will only occur if there is a hydrophilic pore-network for capillary transport of liquid water [58]. Despite these rather contrary interpretations on the functions of MPL in improving water management, the roles of the MPL may include the following [21,27,244,257]: (1) saturated vapor pressure is higher inside the MPL than inside the GDL, due to smaller pore size and enhanced hydrophobicity, rendering the MPL less prone to flooding; (2) the MPL renders the GDL more like a pressure valve with a two-fold function: pushing the water to the membrane side to effectively hydrate the membrane, and providing a pressure buildup necessary to expel the water through the less hydrophobic GDL pores into the cathode flow channels. In addition, under long term operation, the GDL samples are observed to lose their hydrophobicity, fortunately, the presence of an MPL mitigates the loss of hydrophobicity in the macro-porous diffusion media, possibly due to the enhanced liquid resistance induced by the inclusion of MPL [258].

Due to its critical role in improving water management, some research efforts [245,259-261] have focused on investigating the effect of physical properties of the MPL (*i.e.*, carbon black, hydrophobic agent, thickness, etc.) to determine the optimum internal architecture of the MPL and hence the fuel cell performance. Yan *et al.* [262] investigated the physical propertied of the MPL using fluorinated ethylene propylene (FEP) as hydrophobic agent. The results show that the best performance can be achieved by using a GDL with 10% FEP content in the carbon paper and 20% content in the MPL. The Vulcan XC-72R carbon loading of 1 mg/cm^2 in the MPL is sufficiently high to obtain the maximum performance. Park *et al.* [263] adopted nano-fibers and nano-tubes as carbon materials of MPL. This newly made micro-layer showed higher gas permeability and good electric conductivity with similar degree of water management as well as enhanced performance.

In order to highlight its water management function for avoiding electrode flooding and membrane dehydration, the MPL is also called the water management layer (WML) by some researchers [264-267]. Besides, Wang *et al.* [268] proposed a self-humidifying MEA with the active electrode region surrounded by an unactive "water transfer region (WTR)" to achieve effective water management and high performance for PEMFCs. By this configuration, excess water in the cathode was transferred to anode through Nafion membrane to humidify hydrogen.

6.3.4. CL material and structure design

The catalyst layer, placed between the membrane and the GDL, is the core component of the whole MEA, where catalyst particles, polymer electrolyte and pore space form the three-phase region for oxygen reduction reaction to produce water. In water management, the role of the CL should be the

prime component for the conversion of liquid water to vapor and acts like a watershed that regulates the balance between the opposing water fluxes toward the membrane and the GDL [269].

Modification of the microstructures of the catalyst layer has been a newer attempt of MEA material and structure design to address water management in the PEMFC. To reduce the effect of flooding in the CL, Nguyen *et al*. [270] developed a CL structure by first establishing a structure with multiple ionic (Nafion) and electronic (Carbon) interconnected paths for proton and electron transport, and then partially filling the void space with nano-sized hydrophobic particles, which can provide optimal gas and liquid transport paths to and from the CL, while maintaining higher electronic and ionic conductivities. In another example, Wakayama *et al*. [271,272] deposited some magnetic particles in the cathode CL to optimize water management because the magnet particles can decrease the saturation level of liquid water by Kelvin force. But, it is doubtful of the strength of the Kelvin force to enough force the production water out of the CL.

A MnO_2−Pt/C composite electrode was designed to solve the VRE caused by oxygen starvation [41], which was based upon the fact that the electrochemical reduction of MnO_2 has almost the same Nernstian potential as the ORR. It has been found that the MnO_2−Pt/C composite electrode can overcome the voltage reversal effect to a certain extent. Even though the discharged MnO_2 can be recovered after a length of time at rest, the effect of discharged MnO_2 on the MEA is still under question, especially, if MnO_2 is deeply discharged to Mn^{2+} rather than MnOOH, which has capability to return to MnO_2 but Mn^{2+} does not.

Although water flooding has been extensively studied, all measures having been reported so far only partly succeed in solving the water flooding accumulated at the gas flow channels of a bipolar plate but hardly succeed in solving water flooding happening at the pores in the CL and the GDL of a porous electrode. Actually, the pores in CL would be no sooner flooded than the first drop of water was produced at the CL of a PEMFC electrode. Thus, the performance of the PEMFC reported so far was actually discounted by water flooding happening in the catalyst layer of the electrode at the very begining. In order to shorten the distance of the gas diffusion in a water-flooded porous electrode, an ultrathin catalyst layer is often recommended in a PEMFC. That is why the catalyst coated membrane (CCM) technique, in which only a very ultrathin catalyst layer is employed, has prevailed for years. Obviously, an ultrathin catalyst layer sacrifices the electrodes' space efficiency of the PEMFC [40].

PEMFCs can be taken as a device generating electricity and water at the cathode concurrently. Thus water flooding to the cathode seems unavoidable. As a matter of fact, why water flooding is a problem that has to be solved or alleviated is principally due to the extremely low solubility of reactant gases (H_2, O_2) in water, especially at the operation temperature of the PEMFCs, 60 ℃ *ca.* As long as the pores for gas storage and transport were occupied by water, the flux of gas transport to the catalyst surface through the water would be extremely small. The fuel or oxidant starvation would happen. Thus if one can find a media, in which reactant gases (H_2, O_2) have a high solubility, to fill in the pores before water production and water flooding happening, the problem having being harassed us for decades would be solved. Fortunately, the invention developed by Wei's group seems to have successfully solved this problem [40,273-276].

Based on the principle of "like dissolves like", Wei's group developed a novel cathode containing nonpolar water-proof oil, dimethyl-silicon-oil (DMS), which was added into a fraction of pores of a

cathode of a conventional Pt/C electrode (CPE). The solubility of oxygen in such nonpolar water-proof oil DMS is over 60 times higher than that in polar water at the temperature of 60 °C *ca.* Thus, the pores occupied by such nonpolar water-proof oil form unoccupied channels for oxygen transportation, in which the DMS is hardly extruded by water, regardless of whether the cathode is flooded or not. The electrode containing such water-proof oil DMS was named antiflooding electrode (AFE). The performance of the cell with AFE cathode and CPE cathode is illustrated in Figure 10 [40,273,274].

Figure 10. Schematic of processes happening in the CPE and the AFE (a), Cell voltage vs. Time of a MEA with an AFE or CPE as the cathode at a current density of 1A cm^{-2} (b), and Cell voltage and Power density vs. Current density of a single cell (c) with a CPE anode and an AFE cathode in the case of no O_2 humidification (○) and O_2 over-humidification at 156% RH (●), and a single cell with two CPEs in the case of no O_2 humidification (△) and O_2 over-humidification at 156% RH (▲). [40].
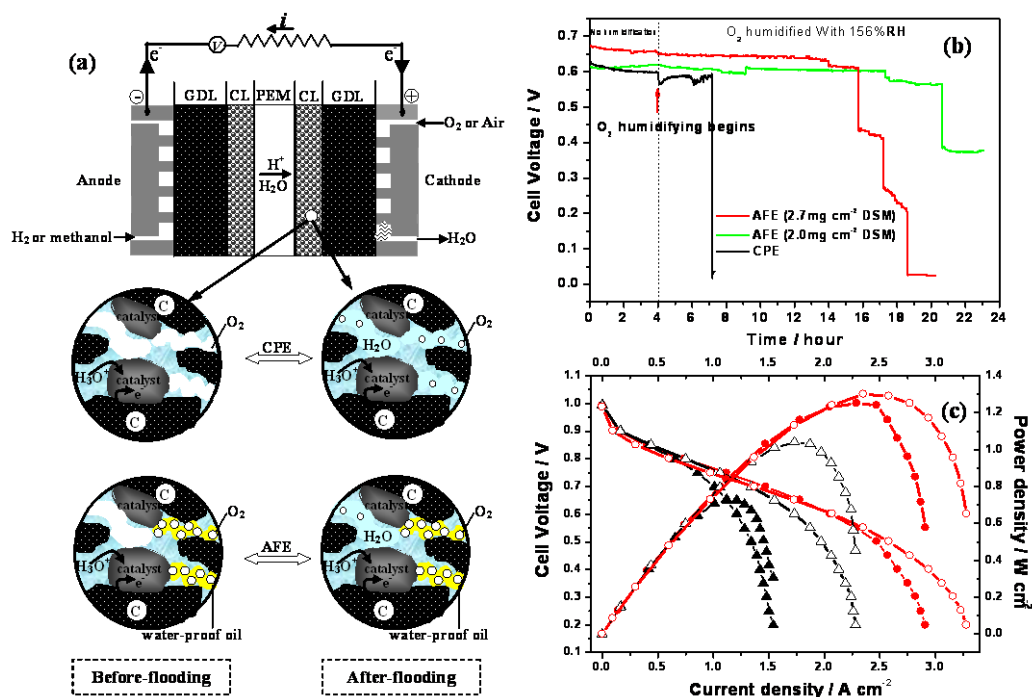
The experiment illustrated in Figure 10(b) was divided into two sections, in the early four hours O_2 was not humidified and in the rest of time O_2 was over-humidified at humidity of 156% RH. The voltage of the cell with an AFE cathode is always greater than the cell with a CPE cathode regardless of O_2 humidification or not. The cell with a CPE cathode only sustained another 2.5 hours and then collapsed after O_2 was over-humidified at humidity of 156% RH. However, the cell with an AFE cathode sustained another 12 and 17 hours before collapse for two cells with different DMS loadings, respectively. It implies that the cell with an AFE cathode wins at least nine hours more life before advent of the VRE than the cell with a CPE cathode in the case of the over-humidity. Figure 10(c) displays cell voltage and power density vs. current density of a single cell with an AFE cathode (○, ●) or a CPE cathode (△, ▲) in two cases, that is, oxygen not humidified and humidified with 156% RH.

From the results disclosed in Figure 10(b) and (c) the following points can be concluded: (1) Regardless of O_2 humidification or not, the performance of a single cell with an AFE cathode is always much better than the cell with a CPE cathode. It means that even at a well-designed operational condition the flooding of produced water to the pores of the cathode can seriously worsen the PEMFC output. Fortunately, the AFE can overcome it. (2) The performance of the MEA with a CPE cathode deteriorates very quickly after O_2 over-humidification but the cell with an AFE cathode can sustain a quite long time without a serious degradation. It means that the pores for gas transportation in the CPE will be predominantly occupied by water in the case of O_2 over-humidification. Most of the loss in a cell's performance is not from the water flooding to the gas channel in the bipolar plate but from the water flooding to the pores in the catalyst layer. (3) The cell performance at a large current density was noticeably improved with the introduction of the AFE into the MEA. For example, in the case of O_2 over-humidification the cell with two CPE can only sustain a current density of 1.5 A.cm^{-2} but the cell with an AFE cathode can sustain a current density as large as 3.0 A.cm^{-2}; in the case of the not-humidified cathode the cell with two CPE can sustain a current density of about 2.3 A.cm^{-2} but the cell with an AFE cathode can sustain a current density as large as 3.3 A.cm^{-2}. The larger the current density is drawn, the more water will be produced, and the more pores for gas transportation will be occupied by water. The difference in the case of the not-humidified cathode once again proves that the flooding to the porous electrode itself rather than the gas channel in the bipolar plate is principally responsible for the deterioration of the PEMFC performance. Thus, solving the flooding to the porous electrode itself means solving almost all problems associated with water flooding. The AFE is just invented for this purpose. Figure 11 tells the difference in pore volumes of a CPE before and after introduction of the DMS. The main difference in pore volumes appears in the pores from 20nm to 70 nm. It suggests that the DMS mainly fills in the pores with meso-diameter from 20 nm to 70 nm. It is the water condensation in the pores with a diameter from 20nm to 70 nm that cause so-called flooding of the electrode. The pores with a diameter below 20 nm may always be occupied by water due to water capillary condensation in such small pores. The pores with a diameter over 70 nm may primarily belong to the gas, and water can be easily excluded because of their hydrophobility even though the large pores are occupied by water. Besides, due to the smaller capillary pressure in pores larger than 70 nm, it is slightly more difficult for water to condense down in such large pores. The water in the pores with a diameter from 20 to 70 nm, however, may be not easily excluded because water capillary condensation in such pores is not as small as that in large pores. The situation will be different if the pores with a diameter from 20 to 70 nm were in advance occupied by oil, such as DMS, which has a zero contact angle with carbon, Nafion and Teflon, but 117 ° contact angle with water. It can be expected that DMS can well penetrate into the pores configured by carbon, Nafion and Teflon. Once the pores are occupied by DMS, the DMS will be hardly extruded by water due to its property of water proof. the authors affirmed that solving the flooding of the pores with a diameter of 20 to 70 nm means solving all problem that have been harassing the PEMFC in water management.

A question will be arise naturally. Does the filling of the DMS to the pores of the cathode overlay any surface of catalysts? The answer is yes, as illustrated in Figure 12 [275,276]. As a saying goes there is no benefit coming without compromise. The partial loss of catalyst surface is the cost of using DMS

in the electrode. However, such a loss seems worthy of overcoming the disastrous consequence of water flooding.

Figure 11. Pore volume distribution of a CPE with an apparent area of 4 cm^2 before (black line) and after (red line) addition of 2.5 mg cm^{-2} DMS [40].
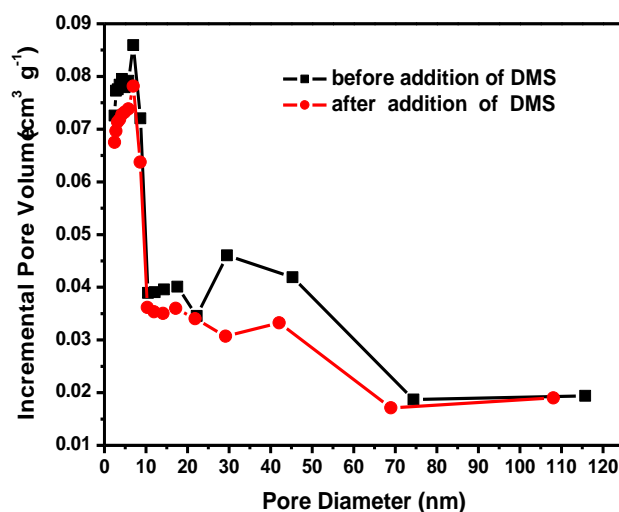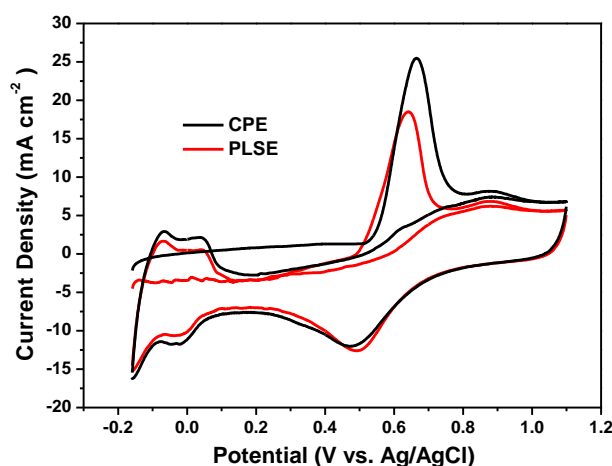

Figure 12. Comparison of CO stripping voltammograms acquired at 10 mV s^{-1} plotted for CPE and AFE in 0.5 mol L^{-1} H$_2$SO$_4$ solution under argon atmosphere at room temperature. Scan rate: 10 mV s^{-1}, the Pt loading for CPE and AFE is 1.5 mg cm^{-2} [273].

7. Conclusions

The major issue impacting the performance and durability of PEM fuel cells, namely the water management, has been methodically reviewed. Large-scale commercialization of PEM fuel cells calls calls for not only lowering the cost, but also increasing the durability and optimizing the cell performance by optimizing the water management. How to find a subtle equilibrium between membrane dehydration and liquid water flooding is the key to achieve optimum water management, which depends on several variables, such as the reactant stream humidification, the flow field layout, the structural and wetting properties of the GDL and MPL. Over the past decade, extensive research works have been

carried out on water management, including visualization of liquid water distribution, prediction through numerical modeling, experimental measurements, and optimum strategies of water management including optimum operational condition, convenient cell system design and MEA material and structure design.

Water management strategies must be addressed with due consideration to the overall system design, to maintain the overall system simplicity and minimize the system parasitic power loss, thereby decreasing the costs and increasing reliability. Of all strategies against water flooding, materials and structures of the MEA should be given more attention because the first drop of water is produced therein, and there is almost no any significant parasitic power loss and on assistant equipment is needed by adjusting materials and structures of the MEA. The separate channels for water and reactant gases transport, specifically, in a porous electrode would be a promising way for the final solution of water flooding harassing PEMFCs.

Acknowledgements

References and Notes

1. Dresselhaus, M.S.; Thomas, I.L. Alternative energy technologies. *Nature* **2001**, *414*, 332-337.
2. Canut, J.M.L.; Abouatallah, R.M.; Harrington, D.A. Detection of membrane drying, fuel cell flooding, and anode catalyst poisoning on PEMFC stacks by electrochemical impedance spectroscopy. *J. Electrochem. Soc.* **2006**, *153*, A857-A864.
3. Nguyen, T.V.; Knobbe, M.W. A liquid water management strategy for PEM fuel cell stacks. *J. Power Sources* **2003**, *114*, 70-79.
4. Zawodzinski, T.A.,Jr.; Springer, T.E.; Davey, J.; Jestel, R.; Lopez, C.; Valerio, J.; Gottesfeld, S. A comparative study of water uptake by and transport through ionomeric fuel cell membranes. *J. Electrochem. Soc.* **1993**, *140*, 1981-1985.
5. Zawodzinski, T.A.,Jr.; Derouin, C.; Radzinski, S.; Sherman, R.J.; Smith, V.T.; Springer, T.E.; Gottesfeld, S. Water uptake by and transport through Nafion 117 membranes. *J. Electrochem. Soc.* **1993**, *140*, 1041-1047.
6. Zawodzinski, T.A.; Davey, J.; Valerio, J.; Gottesfeld, S. The water dependence of electro-osmotic drag in proton-conducting polymer electrolytes. *Electrochim. Acta* **1995**, *40*, 297-302.
7. Janseen, G.J.M.; Overvelde, M.L.J. Water transport in the proton-exchange-membrane fuel cell: Measurements of the effective drag coefficient. *J. Power Sources* **2001**, *101*, 117-125.
8. Sridhar, P. Humidification studies on polymer electrolyte membrane fuel cell. *Fuel Energy Abst.* **2002**, *43*, 262.
9. Hickner, M.A.; Fujimoto, C.H.; Cornelius, C.J. Transport in sulfonated poly (phenylene)s: Proton conductivity, permeability, and the state of water. *Polymer* **2006**, *47*, 4238-4244.

10. Stumper, J.; Löhr, M.; Hamada, S. Diagnostic tools for liquid water in PEM fuel cell. *J. Power Sources* **2005**, *143*, 150-157.

11. Okada, T. Theory for water management in membranes for polymer electrolyte fuel cells: Part 1. The effect of impurity ions at the anode side on the membrane performances. *J. Electroanal. Chem.* **1999**, *465*, 1-17.

12. Knights, S.D.; Colbow, K.M.; St-Pierre, J.; Wilkinson, D.P. Aging mechanisms and lifetime of PEFC and DMFC. *J. Power Sources* **2004**, *127*, 127-134.

13. Sone, Y.; Ekdunge, P.; Simonsson, D. Proton conductivity of Nafion 117 as measured by a four-electrode AC impedance method. *J. Electrochem. Soc.* **1996**, *143*, 1254-1259.

14. Pasaogullari, U.; Wang, C.Y. Two-phase transport in polymer electrolyte fuel cells with bi-layer cathode gas diffusion media. *J. Electrochem. Soc.* **2005**, *152*, A380-A390.

15. Liu, X.; Guo, H.; Ma, C.F. Water flooding and two-phase flow in cathode channels of proton exchange membrane fuel cells. *J. Power Sources* **2006**, *156*, 267-280.

16. Liu, X.; Guo, H.; Ye, F.; Ma, C.F. Water flooding and pressure drop characteristics in flow channels of proton exchange membrane fuel cells. *Electrochim. Acta* **2007**, *52*, 3607-3614.

17. Barbir, F.; Gorgun, H.; Wang, X. Relationship between pressure drop and cell resistance as a diagnostic tool for PEM fuel cells. *J. Power Sources* **2005**, *141*, 96-101.

18. Natarajan, D.; Nguyen, T.V. Current distribution in PEM fuel cells. Part 1: Oxygen and fuel flow rate effects. *AIChE J.* **2005**, *51*, 2587-2598.

19. Meng, H.; Wang, C.Y. New model of two-phase flow and flooding dynamics in polymer electrolyte fuel cells. *J. Electrochem. Soc.* **2005**, *152*, A1733-A1741.

20. Yamada, H.; Hatanaka, T.; Murata, H.; Morimoto, Y. Measurement of flooding in gas diffusion layers of polymer electrolyte fuel cells with conventional flow field. *J. Electrochem. Soc.* **2006**, *153*, A1748-A1754.

21. Spernjak, D.; Prasad, A.K.; Advani, S.G. Experimental investigation of liquid water formation and transport in a transparent single-serpentine PEM fuel cell. *J. Power Sources* **2007**, *170*, 334-344.

22. Wang, C.Y. Fundamental models for fuel cell engineering. *Chem. Rev.* **2004**, *104*, 4727-4766.

23. St-Pierre, J.; Wilkinson, D.P.; Knights, S.; Bos, M. Relationships between water management, contamination and lifetime degradation in PEFC. *J. New Mater. Electrochem. Syst.* **2000**, *3*, 99-106.

24. He, W.S.; Lin, G.Y.; Nguyen, T.V. Diagnostic tool to detect electrode flooding in proton-exchange-membrane fuel cells. *AIChE J.* **2003**, *49*, 3221-3228.

25. Eikerling, M.; Kornyshev, A.A.; Kucernak, A.R. Water in polymer electrolyte fuel cells: Friend or foe? *Phys. Today* **2006**, *59*, 38-44.

26. Yousfi-Steiner, N.; Moçotéguy, P.; Candusso, D.; Hissel, D.; Hernandez, A.; Aslanides, A. A review on PEM voltage degradation associated with water management: Impacts, influent factors and characterization. *J. Power Sources* **2008**, *183*, 260-274.

27. Li, H.; Tang, Y.H.; Wang, Z.W.; Shi, Z.; Wu, S.H.; Song, D.T.; Zhang, J.L.; Fatih, K.; Zhang, J.J.; Wang, H.J.; Liu, Z.S.; Abouatallah, R.; Mazza, A. A review of water flooding issues in the proton exchange membrane fuel cell. *J. Power Sources* **2008**, *178*, 103-117.

28. Rodatz, P.; Büchi, F.; Onder, C.; Guzzella, L. Operational aspects of a large PEFC stack under practical conditions. *J. Power Sources* **2004**, *128*, 208-217.

29. Eckl, R.; Zehtner, W.; Leu, C.; Wagner, U. Experimental analysis of water management in a self-humidifying polymer electrolyte fuel cell stack. *J. Power Sources* **2004**, *138*, 137-144.

30. Schmittinger, W.; Vahidi, A. A review of the main parameters influencing long-term performance and durability of PEM fuel cells. *J. Power Sources* **2008**, *180*, 1-14.

31. Wang, Y.; Wang, C.Y. Dynamics of polymer electrolyte fuel cells undergoing load changes. *Electrochim. Acta* **2006**, *51*, 3924-3933.

32. Li, G.C.; Pickup, P.G. Dependence of electrode overpotentials in PEM fuel cells on the placement of the reference electrode. *Electrochem. Solid-State Lett.* **2006**, *9*, A249-A251.

33. Nguyen, T.V.; White, R.E. A water and heat management model for proton-exchange-membrane fuel cells. *J. Electrochem. Soc.* **1993**, *140*, 2178-2186.

34. Büchi, F.N.; Srinivasan, S. Operating proton exchange membrane fuel cells without external humidification of the reactant gases. *J. Electrochem. Soc.* **1997**, *144*, 2767-2772.

35. Huang, X.Y.; Solasi, R.; Zou, Y.; Feshler, M.; Reifsnider, K.; Condit, D.; Burlatsky, S.; Madden, T. Mechanical endurance of polymer electrolyte membrane and PEM fuel cell durability. *J. Polym. Sci. Part B Polym. Phys.* **2006**, *44*, 2346-2357.

36. Yu, J.R.; Matsuura, T.; Yoshikawa, Y.; Islam, M.N.; Hori, M. *In situ* analysis of performance degradation of a PEMFC under nonsaturated humidification. *Electrochem. Solid-State Lett.* **2005**, *8*, A156-A158.

37. Weber, A.Z.; Newman, J. Modeling transport in polymer-electrolyte fuel cells. *Chem. Rev.* **2004**, *104*, 4679-4726.

38. Um, S.; Wang, C.Y. Computation study of water transport in proton exchange membrane fuel cells. *J. Power Sources* **2006**, *156*, 211-223.

39. Piela, P.; Springer, T.E.; Davey, J.; Zelenay, P. Direct measurement of *iR*-free individual-electrode overpotentials in polymer electrolyte fuel cells. *J. Phys. Chem. C* **2007**, *111*, 6512-6523.

40. Ji, M.B.; Wei, Z.D.; Chen, S.G.; Li, L. A novel anti-flooding electrode for proton exchange membrane fuel cells. *J. Phys. Chem. C* **2009**, *113*, 765-771.

41. Wei, Z.D.; Ji, M.B.; Hong, Y.; Sun, C.X.; Chan, S.H.; Shen, P.K. MnO_2-Pt/C composite electrodes for preventing voltage reversal effects with polymer electrolyte membrane fuel cells. *J. Power Sources* **2006**, *160*, 246-251.

42. Ge, S.H.; Wang, C.Y. Liquid water formation and transport in the PEFC anode. *J. Electrochem. Soc.* **2007**, *154*, B998-B1005.

43. McKay, D.A.; Ott, W.T.; Stefanopoulou, A.G. Modeling, parameter identification, and validation of reactant water dynamics for a fuel cell stack. In *Proceedings of IMECE'05 2005 ASME International Mechanical Engineering Congress & Exposition*; Orlando, FL, USA, November 5-11, 2005.

44. López, A.M.; Barreras, F.; Lozano, A.; García, J.A.; Valiño, L.; Mustata, R. Comparison of water management between two bipolar plate flow-field geometries in proton exchange membrane fuel cells at low-density current range. *J. Power Sources* **2009**, *192*, 94-99.

45. Kim, H.S.; Min, K. Experimental investigation of dynamic responses of a transparent PEM fuel cell to step changes in cell current density with operating temperature. *J. Mech. Sci. Technol.* **2008**, *22*, 2274-2285.

46. Yamauchi, M.; Sugiura, K.; Yamauchi, T.; Taniguchi, T.; Itoh, Y. Proposal for an optimum water management method using two-pole simultaneous measurement. *J. Power Sources* **2009**, *193*, 1-8.

47. Hussaini, I.S.; Wang, C.Y. Visualization and quantification of cathode channel flooding in PEM fuel cells. *J. Power Sources* **2009**, *187*, 444-451.

48. Ma, H.P.; Zhang, H.M.; Hu, J.; Cai, Y.H.; Yi, B.L. Diagnostic tool to detect liquid water removal in the cathode channels of proton exchange membrane fuel cells. *J. Power Sources* **2006**, *162*, 469-473.

49. Tüber, K.; Pócza, D.; Hebling, C. Visualization of water buildup in the cathode of a transparent PEM fuel cell. *J. Power Sources* **2003**, *124*, 403-414.

50. Hakenjos, A.; Muenter, H.; Wittstadt, U.; Hebling, C. A PEM fuel cell for combined measurement of current and temperature distribution, and flow field flooding. *J. Power Sources* **2004**, *131*, 213-216.

51. Borrelli, J.; Kandlikar, S.; Trabold, T.; Owejan, J. Water transport visualization and two-phase pressure drop measurements in a simulated PEMFC cathode minichannel. In *Proceedings of the 3rd International Conference on Microchannels and Minichannels*; Toronto, Ontario, Canada, June 13-15, 2005.

52. Sugiura, K.; Nakata, M.; Yodo, T.; Nishiguchi, Y.; Yamauchi, M.; Itoh, Y. Evaluation of a cathode gas channel with a water absorption layer/waste channel in a PEFC by using visualization technique. *J. Power Sources* **2005**, *145*, 526-533.

53. Kumbur, E.; Sharp, K.; Mench, M. Liquid droplet behavior and instability of a polymer electrolyte fuel cell flow channel. *J. Power Sources* **2006**, *161*, 333-345.

54. Spernjak, D.; Advani, S.; Prasad, A. Experimental investigation of liquid water formation and transport in a transparent single-serpentine PEM fuel cell. *J. Power Sources* **2007**, *170*, 334-344.

55. Weng, F.B.; Su, A.; Hsu, C.Y.; Lee, C.Y. Study of water-flooding behaviour in cathode channel of a transparent proton exchange membrane fuel cell. *J. Power Sources* **2006**, *157*, 674-680.

56. Zhang, F.Y.; Yang, X.G.; Wang, C.Y. Liquid water removal from a polymer electrolyte fuel cell. *J. Electrochem. Soc.* **2006**, *153*, A225-A232.

57. Bazylak, A.; Sinton, D.; Liu, Z.S.; Djilali, N. Effect of compression on liquid water transport and microstructure of PEMFC gas diffusion layers. *J. Power Sources* **2007**, *163*, 784-792.

58. Yang, X.G.; Zhang, F.Y.; Lubawy, A.; Wang, C.Y. Visualization of liquid water transport in a PEFC. *Electrochem. Solid-State Lett.* **2004**, *7*, A408-A411.

59. Theodorakakos, A.; Ous, T.; Gavaises, M.; Nouri, J.; Nikolopoulos, N.; Yanagihara, H. Dynamics of water droplets detached from porous surfaces of relevance to PEM fuel cells. *J. Collo. Interf. Sci.* **2006**, *300*, 673-687.

60. Litster, S.; Sinton, D.; Djilali, N. *Ex situ* visualization of liquid water transport in PEM fuel cell gas diffusion layers. *J. Power Sources* **2006**, *154*, 95-105.

61. Bazylak, A.; Sinton, D.; Djilali, N. Dynamic water transport and droplet emergence in PEMFC gas diffusion layers. *J. Power Sources* **2008**, *176*, 240-246.

62. Kimball, E.; Whitaker, T.; Kevrekidis, Y.; Benziger, J. Drops, slugs, and flooding in polymer electrolyte membrane fuel cells. *Am. Inst. Chem. Eng.* **2008**, *54*, 1313-1332.

63. Lu, Z.; Kandlikar, S.G.; Rath, C.; Grimm, M.; Domigan, W.; White, A.D.; Hardbarger, M.; Owejan, J.P.; Trabold, T.A. Water management studies in PEM fuel cells, Part II: *ex situ* investigation of flow maldistribution, pressure drop and two-phase flow pattern in gas channels. *Int. J. Hydrogen Energy* **2009**, *34*, 3445-3456.

64. Gao, B.; Steenhuis, T.; Zevi, Y.; Parlange, J.-Y.; Carter, R.; Trabold, T. Visualization of unstable water flow in a fuel cell gas diffusion layer. *J. Power Sources* **2009**, *190*, 493-498.

65. Perrin, J.C.; Lyonnard, S.; Guillermo, A.; Levitz, P. Water dynamics in ionomer membranes by field-cycling NMR relaxometry. *J. Phys. Chem. B* **2006**, *110*, 5439-5444.

66. Zhang, Z.H.; Martin, J.; Wu, J.F.; Wang, H.J.; Promislow, K.; Balcom, B.J. Magnetic resonance imaging of water content across the Nafion membrane in an operation PEM fuel cell. *J. Magn. Reson.* **2008**, *193*, 259-266.

67. Tsushima, S.; Hirai, S.; Kitamura, K.; Yamashita, M.; Takasel, S. MRI application for clarifying fuel cell performance with variation of polymer electrolyte membranes: comparison of water content of a hydrocarbon membrane and a perfluorinated membrane. *Appl. Magn. Res.* **2007**, *32*, 233-241.

68. Dunbar, Z.; Masel, R. Quantitative MRI study of water distribution during operation of a PEM fuel cell using Teflon flow fields. *J. Power Sources* **2007**, *171*, 678-687.

69. Feindel, K.W.; Bergens, S.H.; Wasylishen, R.E. Use of hydrogen–deuterium exchange for contrast in ^{1}H NMR microscopy investigations of an operating PEM fuel cell. *J. Power Sources* **2007**, *173*, 86-95.

70. Feindel, K.W.; Bergens, S.H.; Wasylishen, R.E. The influence of membrane electrode assembly water content on the performance of a polymer electrolyte membrane fuel cell as investigated by ^{1}H NMR microscopy. *Phys. Chem. Chem. Phys.* **2007**, *9*, 1850-1857.

71. Feindel, K.W.; Bergens, S.H.; Wasylishen, R.E. The use of ^{1}H NMR microscopy to study proton-exchange membrane fuel cells. *Chem. Phys. Chem.* **2006**, *7*, 67-75.

72. Feindel, K.W.; Bergens, S.H.; Wasylishen, R.E. Insights into the distribution of water in a self-humidifying H_2/O_2 proton-exchange membrane fuel cell using ^{1}H NMR microscopy. *J. Am. Chem. Soc.* **2006**, *128*, 14192-14199.

73. Feindel, K.W.; LaRocque, L.P.A.; Starke, D.; Bergens, S.H.; Wasylishen, R.E. In situ observations of water production and distribution in an operating H_2/O_2 PEM fuel cell assembly using ^{1}H NMR microscopy. *J. Am. Chem. Soc.* **2004**, *126*, 11436-11437.

74. Minard, K.; Viswanathan, V.; Majors, P.; Wang, L.; Rieke, P. Magnetic resonance imaging (MRI) of PEM dehydration and gas manifold flooding during continuous fuel cell operation. *J. Power Sources* **2006**, *161*, 856-863.

75. Teranishi, K.; Tsushima, S.; Hirai, S. Analysis of water transport in PEFCs by magnetic resonance imaging measurement. *J. Electrochem. Soc.* **2006**, *153*, A664-A668.

76. Teranishi, K.; Tsushima, S.; Hirai, S. Study of the effect of membrane thickness on the performance of polymer electrolyte fuel cells by water distribution in a membrane. *Electrochem. Solid-State Lett.* **2005**, *8*, A281-A284.

77. Tsushima, S.; Teranishi, K.; Hirai, S. Water diffusion measurement in fuel-cell SPE membrane by NMR. *Energy* **2005**, *30*, 235-245.

78. Tsushima, S.; Teranishi, K.; Nishida, K.; Hirai, S. Water content distribution in a polymer electrolyte membrane for advanced fuel cell system with liquid water supply. *Magn. Reson. Imaging* **2005**, *23*, 255-258.

79. Tsushima, S.; Teranishi, K.; Hirai, S. Magnetic resonance imaging of the water distribution within a polymer electrolyte membrane in fuel cells. *Electrochem. Solid-State Lett.* **2004**, *7*, A269-A272.

80. Hartnig, C.; Manke, I.; Kardjilov, N.; Hilger, A.; Grünerbel, M.; Kaczerowski, J.; Banhart, J.; Lehnert, W. Combined neutron radiography and locally resolved current density measurements of operating PEM fuel cells. *J. Power Sources* **2008**, *176*, 452-459.

81. Kim, T.J.; Kim, J.R.; Sim, C.M.; Lee, S.W.; Kaviany, M.; Son, S.Y.; Kim, M.H. Experimental approaches for distribution and behavior of water in PEMFC under flow direction and differential pressure using neutron imaging technique. *Nucl. Instr. and Meth. Phys. Res. Sec. A* **2009**, *600*, 325-327.

82. Gebel, G.; Diat, O. Neutron and X-ray scattering: suitable tools for studying ionomer membranes. *Fuel Cells* **2005**, *5*, 261-276.

83. Gagliardo, J.J.; Owejan, J.P.; Trabold, T.A.; Tighe, T.W. Neutron radiography characterization of an operating proton exchange membrane fuel cell with localized current distribution measurements. *Nucl. Instr. Meth. Phys. Res. Sec. A* **2009**, *605*, 115-118.

84. Owejan, J.P.; Gagliardo, J.J.; Sergi, J.M.; Kandlikar, S.G.; Trabold, T.A. Water management studies in PEM fuel cells, Part I: Fuel cell design and in situ water distributions. *Int. J. Hydrogen Energy* **2009**, *34*, 3436-3444.

85. Gebel, G.; Diat, O.; Escribano, S.; Mosdale, R. Water profile determination in a running PEMFC by small-angle neutron scattering. *J. Power Sources* **2008**, *179*, 132-139.

86. Kim, S.; Mench, M.M. Investigation of temperature-driven water transport in polymer electrolyte fuel cell: phase-change-induced flow. *J. Electrochem. Soc.* **2009**, *156*, B353-B362.

87. Kim, T.J.; Sim, C.M.; Kim, M.H. Research on water discharge characteristics of PEM fuel cells by using neutron imaging technology at the NRF, HANARO. *Appl. Radiat. Isot.* **2008**, *66*, 593-605.

88. Park, J.; Li, X.G.; Tran, D.; Abdel-Baset, T.; Hussey, D.S.; Jacobson, D.L.; Arif, M. Neutron imaging investigation of liquid water distribution in and the performance of a PEM fuel cell. *Int. J. Hydrogen Energy* **2008**, *33*, 3373-3384.

89. Hussey, D.; Jacobson, D.; Arif, M.; Owejan, J.; Gagliardo, J.; Trabold, T. Neutron images of the through-plane water distribution of an operating PEM fuel cell. *J. Power Sources* **2007**, *172*, 225-228.

90. Chen, Y.S.; Peng, H.; Hussey, D.S.; Jacobson, D.L.; Tran, D.T.; Abdel-Baset, T.; Biernacki, M. Water distribution measurement for a PEMFC through neutron radiography. *J. Power Sources* **2007**, *170*, 376-386.

91. Owejan, J.P.; Trabold, T.A.; Gagliardo, J.J.; Jacobson, D.L.; Carter, R.N.; Hussey, D.S.; Arif, M. Voltage instability in a simulated fuel cell stack correlated to cathode water accumulation. *J. Power Sources* **2007**, *171*, 626-633.

92. Hickner, M.A.; Siegel, N.P.; Chen, K.S.; McBrayer, D.N.; Hussey, D.S.; Jacobson, D.L.; Arif, M. Real-time imaging of liquid water in an operating proton exchange membrane fuel cell. *J. Electrochem. Soc.* **2006**, *153*, A902-A908.

93. Ludlow, D.J.; Calebrese, C.M.; Yu, S.H.; Dannehy, C.S.; Jacobson, D.L.; Hussey, D.S.; Arif, M.; Jensen, M.K.; Eisman, G.A. PEM fuel cell membrane hydration measurement by neutron imaging. *J. Power Sources* **2006**, *162*, 271-278.

94. Bellows, R.; Lin, M.; Arif, M.; Thompson, A.; Jacobson, D. Neutron imaging technique for in situ measurement of water transport gradients within nafion in polymer electrolyte fuel cells. *J. Electrochem. Soc.* **1999**, *146*, 1099-1103.

95. Siegel, J.B.; Mckay, D.A.; Stefanopoulou, A.G.; Hussey, D.S.; Jacobson, D.L. Measurement of liquid water accumulation in a PEMFC with dead-ended anode. *J. Electrochem. Soc.* **2008**, *155*, B1168-B1178.

96. Turhan, A.; Heller, K.; Brenizer, J.S.; Mench, M.M. Passive control of liquid water storage and distribution in a PEFC through flow-field design. *J. Power Sources* **2008**, *180*, 773-783.

97. Zhang, J.B.; Kramer, D.; Shimoi, R.; Ono, Y.; Lehmann, E.; Wokaun, A.; Shinohara, K.; Scherer, G.G. In situ diagnostic of two-phase flow phenomena in polymer electrolyte fuel cells by neutron imaging: Part B. Material variations. *Electrochim. Acta* **2006**, *51*, 2715-2727.

98. Turhan, A.; Heller, K.; Brenizer, J.; Mench, M. Quantification of liquid water accumulation and distribution in a polymer electrolyte fuel cell using neutron imaging. *J. Power Sources* **2006**, *160*, 1195-1203.

99. Trabold, T.A.; Owejan, J.P.; Jacobson, D.L.; Arif, M.; Huffman, P.R. In situ investigation of water transport in an operating PEM fuel cell using neutron radiography: Part 1–Experimental method and serpentine flow field results. *Int. J. Heat Mass Transfer* **2006**, *49*, 4712-4720.

100. Owejan, J.P.; Trabold, T.A.; Jacobson, D.L.; Baker, D.R.; Hussey, D.S.; Arif, M. In situ investigation of water transport in an operating PEM fuel cell using neutron radiography: Part 2–Transient water accumulation in an interdigitated cathode flow field. *Int. J. Heat Mass Transfer* **2006**, *49*, 4721-4731.

101. Kowal, J.; Turhan, A.; Heller, K.; Brenizer, J.; Mench, M. Liquid water storage, distribution, and removal from diffusion media in PEFCs. *J. Electrochem. Soc.* **2006**, *153*, A1971-A1978.

102. Pekula, N.; Heller, K.; Chuang, P.A.; Turhan, A.; Mench, M.M.; Brenizer, J.S.; Ünlü. Study of water distribution and transport in a polymer electrolyte fuel cell using neutron imaging. *Nucl. Instr. Meth. Phys. Res. Sec. A* **2005**, *542*, 134-141.

103. Kramer, D.; Zhang, J.B.; Shimoi, R.; Lehmann, E.; Wokaun, A.; Shinohara, K.; Scherer, G.G. In situ diagnostic of two-phase flow phenomena in polymer electrolyte fuel cells by neutron imaging: Part A. Experimental, data treatment, and quantification. *Electrochim. Acta* **2005**, *50*, 2603-2614.

104. Kramer, D.; Lehmann, E.; Frei, G.; Vontobel, P.; Wokaun, A.; Scherer, G. An on-line study of fuel cell behavior by thermal neutrons. *Nucl. Instr. and Meth. Phys. Res. Sec. A* **2005**, *542*, 52-60.

105. Satija, R.; Jacobson, D.; Arif, M.; Werner, S. In situ neutron imaging technique for evaluation of water management systems in operating PEM fuel cells. *J. Power Sources* **2004**, *129*, 238-245.

106. Mosdale, R.; Gebel, G.; Pineri, M. Water profile determination in a running proton exchange membrane fuel cell using small angle neutron scattering. *J. Membrane Sci.* **1996**, *118*, 269-277.

107. Yu, L.-J.; Chen, W.-C.; Qin, M.-J.; Ren, G.-P. Experimental research on water management in proton exchange membrane fuel cells. *J. Power Sources* **2009**, *189*, 882-887.

108. Nam, J.H.; Lee, K.J.; Hwang, G.S.; Kim, C.J.; Kaviany, M. Microporous layer for water morphology control in PEMFC. *Int. J. Heat Mass Transfer* **2009**, *52*, 2779-2791.

109. Nam, J.H.; Kaviany, M. Effective diffusivity and water-saturation distribution in single- and two-layer PEMFC diffusion medium. *Int. J. Heat Mass Transfer* **2003**, *46*, 4595-4611.

110. Lim, C.; Wang, C.Y. Effects of hydrophobic polymer content in GDL in power performance of a PEM fuel cell. *Electrochim. Acta* **2004**, *49*, 4149-4156.

111. Isopo, A.; Albertini, R. An original laboratory X-ray diffraction method for *in situ* investigations on the water dynamics in a fuel cell proton exchange membrane. *J. Power Sources* **2008**, *184*, 23-28.

112. Lee, S.J.; Lim, N.Y.; Kim, S.; Park, G.G.; Kim, C.S. X-ray imaging of water distribution in a polymer electrolyte fuel cell. *J. Power Sources* **2008**, *185*, 867-870.

113. Sinha, P.; Halleck, P.; Wang, C.Y. Quantification of liquid water saturation in a PEM fuel cell diffusion medium using X-ray microtomography. *Electrochem. Solid-State Lett.* **2006**, *9*, A244-A248.

114. Manke, I.; Hartnig, C.; Grünerbel, M.; Lehnert, W.; Kardjilov, N.; Haibel, A.; Banhart, J.; Riesemeier, H. Investigation of water evolution and transport in fuel cells with high resolution synchrotron X-ray radiography. *Appl. Phys. Lett.* **2007**, *90*, 174105:1–174105:3.

115. Mukaide, T.; Mogi, S.; Yamamoto, J.; Morita, A.; Koji, S.; Takada, K.; Uesugi, K.; Kajiwara, K.; Noma, T. In situ observation of water distribution and behaviour in a polymer electrolyte fuel cell by synchrotron X-ray imaging. *J. Synchrotron Rad.* **2008**, *15*, 329-334.

116. Hartnig, C.; Manke, I.; Kuhn, R.; Kardjilov, N.; Banhart, J.; Lehnert, W. Cross-sectional insight in the water evolution and transport in polymer electrolyte fuel cells. *Appl. Phys. Lett.* **2008**, *92*, 134106:1–134106:3.

117. Bazylak, A. Liquid water visualization in PEM fuel cells: A review. *Int. J. Hydrogen Energy* **2009**, *34*, 3845-3857.

118. Litster, S.; Sinton, D.; Djilali, N. *Ex situ* visualization of liquid water transport in PEM fuel cell gas diffusion layers. *J. Power Sources* **2006**, *154*, 95-105.

119. Xu, F.; Diat, O.; Gebel, G.; Morin, A. Determination of transverse water concentration profile through MEA in a fuel cell using neutron scattering. *J. Electrochem. Soc.* **2007**, *154*, B1389-B1398.

120. Manke, I.; Hartnig, C.; Grünerbel, M.; Kaczerowski, J.; Lehnert, W.; Kardjilov, N.; Hilger, A.; Banhart, J.; Treimer, W.; Strobl, M. Quasi-*in situ* neutron tomography on polymer electrolyte membrane fuel cell stacks. *Appl. Phys. Lett.* **2007**, *90*, 184101-1–184101-3.

121. Li, X.G.; Sabir, I.; Park, J. A flow channel design procedure for PEM fuel cells with effective water removal. *J. Power Sources* **2007**, *163*, 933-942.

122. Owejan, J.P.; Trabold, T.A.; Jacobson, D.L.; Arif, M.; Kandlikar, S.G. Effects of flow field and diffusion layer properties on water accumulation in a PEM fuel cell. *Int. J. Hydrogen Energy* **2007**, *32*, 4489-4502.

123. Gurau, V.; Bluemle, M.J.; De Castro, E.S.; Tsou, Y.M.; Mann, J.A.; Zawodzinski, T.A. Characterization of transport properties in gas diffusion layers for proton exchange membrane fuel cells - 1. Wettability (internal contact angle to water and surface energy of GDL fibers). *J. Power Sources* **2006**, *160*, 1156-1162.

124. Albertini, V.R.; Paci, B.; Generosi, A.; Panero, S.; Navarra, M.A.; di Michiel, M. *In situ* XRD studies of the hydration degree of the polymeric membrane in a fuel cell. *Electrochem. Solid-State Lett.* **2007**, *7*, A519-A521.

125. Ju, H.; Luo, G.; Wang, C.Y. Probing liquid water saturation in diffusion media of polymer electrolyte fuel cells. *J. Electrochem. Soc.* **2007**, *154*, B218-B228.

126. Shimpalee, S.; Greenway, S.; Spuckler, D.; Van Zee, J.W. Predicting water and current distributions in a commercial-size PEMFC. *J. Power Sources* **2004**, *135*, 79-87.

127. Shan, Y.Y.; Choe, S.Y. A high dynamic PEM fuel cell model with temperature effects. *J. Power Sources* **2005**, *145*, 30-39.

128. Haddad, A.; Bouyekhf, R.; Moudni, A.E. Dynamic modeling and water management in proton exchange membrane fuel cell. *Int. J. Hydrogen Energy* **2008**, *33*, 6239-6252.

129. Serincan, M.F.; Yesilyurt, S. Transient analysis of proton electrolyte membrane fuel cells (PEMFC) at start-up and failure. *Fuel Cells* **2007**, *7*, 118-127.

130. Li, A.D.; Zhou, B. A general model of proton exchange membrane fuel cell. *J. Power Sources* **2008**, *182*, 197-222.

131. Wang, Y.; Wang, C.Y. Transient analysis of polymer electrolyte fuel cells. *Electrochim. Acta* **2005**, *50*, 1307-1315.

132. Chen, Y.S.; Peng, H. A segmented model for studying water transport in a PEMFC. *J. Power Sources* **2008**, *185*, 1179-1192.

133. You, L.X.; Liu, H.T. A two-phase flow and transport model for PEM fuel cells. *J. Power Sources* **2006**, *155*, 219-230.

134. Chen, F.; Chang, M.S.; Fang, C.F. Analysis of water transport in a five-layer model of PEMFC. *J. Power Sources* **2007**, *164*, 649-658.

135. Zhang, L.Y.; Pan, M.; Quan, S.H. Model predictive control of water management in PEMFC. *J. Power Sources* **2008**, *180*, 322-329.

136. Ahmed, D.H.; Sung, H.J.; Bae, J.; Lee, D.R. Reactants flow behavior and water management for different current densities in PEMFC. *Int. J. Heat Mass Transfer* **2008**, *51*, 2006-2019.

137. Lum, K.W.; McGuirk, J.J. Three-dimensional model of a complete polymer electrolyte membrane fuel cell-model formulation, validation and parametric studies. *J. Power Sources* **2005**, *143*, 103-124.

138. Shimpalee, S.; Beuscher, U.; Van Zee, J.W. Analysis of GDL flooding effects on PEMFC performance. *Electrochim. Acta* **2007**, *52*, 6748-6754.

139. Baschuk, J.J.; Li, X.G. Modeling of polymer electrolyte membrane fuel cells with variable degrees of water flooding. *J. Power Sources* **2000**, *86*, 181-196.

140. Paquin, M.; Fréchette, L.G. Understanding cathode flooding and dry-out for water management in air breathing PEM fuel cells. *J. Power Sources* **2008**, *180*, 440-451.

141. Natarajan, D.; Nguyen, T.V. Three-dimensional effects of liquid water flooding in the cathode of a PEM fuel cell. *J. Power Sources* **2003**, *115*, 66-80.

142. Wang, Y.; Wang, C.Y. A nonisothermal, two-phase model for polymer electrolyte fuel cells. *J. Electrochem. Soc.* **2006**, *153*, A1193-A1200.

143. Shah, A.A.; Kim, G.S.; Gervais, W.; Young, A.; Promislow, K.; Li, J.; Yi, S. The effects of water and microstructure on the performance of polymer electrolyte fuel cells. *J. Power Sources* **2006**, *160*, 1251-1268.

144. Lin, G.Y.; He, W.S.; Nguyen, T.V. Modeling liquid water effects in the gas diffusion and catalyst layers of the cathode of a PEM fuel cell. *J. Electrochem. Soc.* **2004**, *151*, A1999-A2006.

145. Wu, H.; Li, X.G.; Berg, P. Numerical analysis of dynamic processes in fully humidified PEM fuel cells. *Int. J. Hydrogen Energy* **2006**, *32*, 2022-2031.

146. Liu, Z.X.; Mao, Z.Q.; Wang, C. A two dimensional partial flooding model for PEMFC. *J. Power Sources* **2006**, *158*, 1229-1239.

147. Zhang, Z.G.; Xiao, J.S.; Li, D.Y.; Pan, M.; Yuan, R.Z. Effects of porosity distribution variation on the liquid water flux through gas diffusion layers of PEM Fuel cells. *J. Power Sources* **2006**, *160*, 1041-1048.

148. Karimi, G.; Jafarpour, F.; Li, X. Characterization of flooding and two-phase flow in polymer electrolyte membrane fuel cell stacks. *J. Power Sources* **2009**, *187*, 156-164.

149. Zamel, N.; Li, X.G. A parametric study of multi-phase and multi-species transport in the cathode of PEM fuel cells. *Int. J. Energy Res.* **2008**, *32*, 698-721.

150. Yan, W.M.; Chen, F.L.; Wu, H.Y.; Soong, C.Y.; Chu, H.S. Analysis of thermal and water management with temperature-dependent diffusion effects in membrane of proton exchange membrane fuel cells. *J. Power Sources* **2004**, *129*, 127-137.

151. Karimi, G.; Li, X. Electroosmotic flow through polymer electrolyte membranes in PEM fuel cells. *J. Power Sources* **2005**, *140*, 1-11.

152. Falcão, D.S.; Oliveira, V.B.; Rangel, C.M.; Pinho, C.; Pinto, A.M.F.R. Water transport through a PEM fuel cell: A one-dimensional model with heat transfer effects. *Chem. Eng. Sci.* **2009**, *64*, 2216-2225.

153. Matamoros, L.; Brüggemann, D. Simulation of the water and heat management in proton exchange membrane fuel cells. *J. Power Sources* **2006**, *161*, 203-213.

154. Wang, Y.; Basu, S.; Wang, C.Y. Modeling two-phase flow in PEM fuel cell channels. *J. Power Sources* **2008**, *179*, 603-617.

155. Wang, Z.H.; Wang, C.Y.; Chen, K.S. Two-phase flow and transport in the air cathode of proton exchange membrane fuel cells. *J. Power Sources* **2001**, *94*, 40-50.

156. Zhu, X.; Sui, P.C.; Djilali, N. Dynamic behaviour of liquid water emerging from a GDL pore into a PEMFC gas flow channel. *J. Power Sources* **2007**, *172*, 287-295.

157. Zhu, X.; Sui, P.C.; Djilali, N. Three-dimensional numerical simulations of water droplet dynamics in a PEMFC gas channel. *J. Power Sources* **2008**, *181*, 101-115.

158. Chen, K.S.; Hickner, M.A.; Noble, D.R. Simplified models for predicting the onset of liquid water droplet instability at the gas diffusion layer/gas flow channel interface. *Int. J. Energy Res.* **2005**, *29*, 1113-1132.

159. Golpaygan, A.; Ashgriz, N. Effects of oxidant fluid properties on the mobility of water droplets in the channels of PEM fuel cell. *Int. J. Energy Res.* **2005**, *29*, 1027-1040.

160. He, W.S.; Yi, J.S.; Nguyen, T.V. Two-phase flow model of the cathode of PEM fuel cells using interdigitated flow fields. *AIChE J.* **2000**, *46*, 2053-2064.

161. Bao, C.; Ouyang, M.G.; Yi, B.L. Analysis of thewater and thermal management in proton exchange membrane fuel cell systems. *Int. J. Hydrogen Energy* **2006**, *31*, 1040-1057.

162. Zhou, B.; Huang, W.B.; Zong, Y.; Sobiesiak, A. Water and pressure effects on a single PEM fuel cell. *J. Power Sources* **2006**, *155*, 190-202.

163. Karnik, A.Y.; Stefanopoulou, A.G.; Sun, J. Water equilibria and management using a two-volume model of a polymer electrolyte fuel cell. *J. Power Sources* **2007**, *164*, 590-605.

164. Hassan, N.S.M.; Daud, W.R.W.; Sopian, K.; Sahari, J. Water management in a single cell proton exchange membrane fuel cells with a serpentine flow field. *J. Power Sources* **2009**, *193*, 249-257.

165. Ahmed, D.H.; Sung, H.J. Design of a deflected membrane electrode assembly for PEMFCs. *Int. J. Heat Mass Transfer* **2008**, *51*, 5443-5453.

166. Ahmed, D.H.; Sung, H.J.; Bae, J. Effect of GDL permeability on water and thermal management in PEMFCs — II. Clamping force. *Int. J. Hydrogen Energ.* **2008**, *33*, 3786-3800.

167. Ahmed, D.H.; Sung, H.J. Effects of channel geometrical configuration and shoulder width on PEMFC performance at high current density. *J. Power Sources* **2006**, *162*, 327-339.

168. Ahmed, D.H.; Sung, H.J. Local current density and water management in PEMFCs. *Int. J. Heat Mass Transfer* **2007**, *50*, 3376-3389.

169. Siegel, C. Review of computational heat and mass transfer modeling in polymer-electrolyte-membrane (PEM) fuel cells. *Energy* **2008**, *33*, 1331-1352.

170. Quick, C.; Ritzinger, D.; Lehnert, W.; Hartnig, C. Characterization of water transport in gas diffusion media. *J. Power Sources* **2009**, *190*, 110-120.

171. Colinart, T.; Chenu, A.; Didierjean, S.; Lottin, O.; Besse, S. Experimental study on water transport coefficient in Proton Exchange Membrane Fuel Cell. *J. Power Sources* **2009**, *190*, 230-240.

172. Wang, F.M.; Steinbrenner, J.E.; Hidrovo, C.H.; Kramer, T.A.; Lee, E.S.; Vigneron, S.; Cheng, C.H.; Eaton, J.K.; Goodson, K.E. Investigation of two-phase transport phenomena in microchannels using a microfabricated experimental structure. *Appl. Therm. Eng.* **2007**, *27*, 1728-1733.

173. Kandlikar, S.G.; Lu, Z.; Domigan, W.E.; White, A.D.; Benedict, M.W. Measurement of flow maldistribution in parallel channels and its application to ex-situ and in-situ experiments in PEMFC water management studies. *Int. J. Heat Mass Transfer* **2009**, *52*, 1741-1752.

174. Lu, Z.; Kandlikar, S.G.; Rath, C.; Grimm, M.; Domigan, W.; White, A.D.; Hardbarger, M.; Owejan, J.P.; Trabold, T.A. Water management studies in PEM fuel cells, Part II: Ex situ investigation of flow maldistribution, pressure drop and two-phase flow pattern in gas channels. *Int. J. Hydrogen Energy* **2009**, *34*, 3445-3456.

175. Murahashi, T.; Naiki, M.; Nishiyama, E. Water transport in the proton exchange-membrane fuel cell: Comparison of model computation and measurements of effective drag. *J. Power Sources* **2006**, *162*, 1130-1136.

176. Stumper, J.; Campbell, S.A.; Wilkinson, D.P.; Johnson, M.C.; Davis, M. *In-situ* methods for the determination of current distributions in PEM fuel cells. *Electrochim. Acta* **1998**, *43*, 3773-3783.

177. Fairweather, J.D.; Cheung, P.; St-Pierre, J.; Schwartz, D.T. A microfluidic approach for measuring capillary pressure in PEMFC gas diffusion layers. *Electrochem. Commun.* **2007**, *9*, 2340-2345.

178. Gostick, J.T.; Fowler, M.W.; Ioannidis, M.A.; Pritzker, M.D.; Volfkovich, Y.M.; Sakars, A. Capillary pressure and hydrophilic porosity in gas diffusion layers for polymer electrolyte fuel cells. *J. Power Sources* **2006**, *156*, 375-387.

179. Gostick, J.T.; Ioannidis, M.A.; Fowler, M.W.; Pritzker, M.D. Direct measurement of the capillary pressure characteristics of water-air-gas diffusion layer systems for PEM fuel cells. *Electrochem. Commun.* **2008**, *10*, 1520-1523.

180. Fouquet, N.; Doulet, C.; Nouillant, C.; Dauphin-Tanguy, G.; Ould-Bouamama, B. Model based PEM fuel cell state-of-health monitoring via ac impedance measurements. *J. Power Sources* **2006**, *159*, 905-913.

181. Dai, W.; Wang, H.J.; Yuan, X.Z.; Martin, J.J.; Luo, Z.P.; Pan, M. Measurement of the water transport rate in a proton exchange membrane fuel cell and the influence of the gas diffusion layer. *J. Power Sources* **2008**, *185*, 1267-1271.

182. Ito, K.; Ashikaga, K.; Masuda, H.; Oshima, T.; Kakimoto, Y.; Sasaki, K. Estimation of flooding in PEMFC gas diffusion layer by differential pressure measurement. *J. Power Sources* **2008**, *175*, 732-738.

183. Yoon, Y.G.; Lee, W.Y.; Yang, T.H.; Park, G.G.; Kim, C.S. Current distribution in a single cell of PEMFC. *J. Power Sources* **2003**, *118*, 193-199.

184. Hottinen, T.; Himanen, O.; Lund, P. Effect of cathode structure on planar free-breathing PEMFC. *J. Power Sources* **2004**, *138*, 205-210.

185. Santarelli, M.G.; Torchio, M.F. Experimental analysis of the effects of the operating variables on the performance of a single PEMFC. *Energ. Conv. Manage*. **2007**, *48*, 40-51.

186. Liu, Z.X.; Yang, L.Z.; Mao, Z.Q.; Zhuge, W.L.; Zhang, Y.J.; Wang, L.S. Behavior of PEMFC in starvation. *J. Power Sources* **2006**, *157*, 166-176.

187. Cha, S.W.; O'Hayre, R.; Park, Y.I.; Prinz, F.B. Electrochemical impedance investigation of flooding in micro-flow channels for proton exchange membrane fuel cells. *J. Power Sources* **2006**, *161*, 138-142.

188. Kimball, E.; Whitaker, T.; Kevrekidis, Y.G.; Benziger, J.B. Drops, slugs, and flooding in polymer electrolyte membrane fuel cells. *AIChE J.* **2008**, *54*, 1313-1332.

189. Buaud, F.; Lilandais, D.; Auvity, B. Evidence of a non-dimensional parameter controlling the flooding of PEMFC stack. *Int. J. Hydrogen Energ.* **2008**, *33*, 2765-2773.

190. Nguyen, T.V.; Knobbe, M.W. A liquid water management strategy for PEM fuel cell stacks. *J. Power Sources* **2003**, *114*, 70-79.

191. Knobbe, M.W.; He, W.; Chong, P.Y.; Nguyen, T.V. Active gas management for PEM fuel cell stacks. *J. Power Sources* **2004**, *138*, 94-100.

192. Voss, H.H.; Wilkinson, D.P.; Pickup, P.G.; Johnson, M.C.; Basura, V. Anode water removal: A water management and diagnostic technique for solid polymer fuel cells. *Electrochim. Acta* **1995**, *40*, 321-328.

193. Hanke-Rauschenbach, R.; Mangold, M.; Sundmacher, K. Bistable current-voltage characteristics of PEM fuel cells operated with reduced feed stream humidification. *J. Electrochem. Soc.* **2008**, *155*, B97-B107.

194. Hyun, D.; Kim, J. Study of external humidification method in proton exchange membrane fuel cell. *J. Power Sources* **2004**, *126*, 98-103.

195. Wood, D.L.,III; Yi, J.S.; Nguyen, T.V. Effect of direct liquid water injection and interdigitated flow field on the performance of proton exchange membrane fuel cells. *Electrochim. Acta* **1998**, *43*, 3795-3809.

196. Jung, S.H.; Kim, S.L.; Kim, M.S.; Park, Y.S.; Lim, T.W. Experimental study of gas humidification with injectors for automotive PEM fuel cell systems. *J. Power Sources* **2007**, *170*, 324-333.

197. Soler, J.; Hontañón; Daza, L. Electrode permeability and flow-field configuration: influence on the performance of a PEMFC. *J. Power Sources* **2003**, *118*, 172-178.

198. Nguyen, T.V. A gas distributor design for proton-exchange-membrane fuel cells. *J. Electrochem. Soc.* **1996**, *143*, L103-L105.

199. Merida, W.R.; McLean, G.; Djilali, N. Non-planar architecture for proton exchange membrane fuel cells. *J. Power Sources* **2001**, *102*, 178-185.

200. Kanezaki, T.; Li, X.G.; Baschuk, J.J. Cross-leakage flow between adjacent flow channels in PEM fuel cells. *J. Power Sources* **2006**, *162*, 415-425.

201. Park, J.; Li, X.G. An experimental and numerical investigation on the cross flow through gas diffusion layer in a PEM fuel cell with a serpentine flow channel. *J. Power Sources* **2007**, *163*, 853-863.

202. Xu, C.; Zhao, T.S. A new flow field design for polymer electrolyte-based fuel cells. *Electrochem. Commun.* **2007**, *9*, 497-503.

203. Jang, J.H.; Yan, W.M.; Li, H.Y.; Chou, Y.C. Humidity of reactant fuel on the cell performance of PEM fuel cell with baffle-blocked flow field designs. *J. Power Sources* **2006**, *159*, 468-477.

204. Metz, T.; Paust, N.; Müller, C.; Zengerle, R.; Koltay, P. Passive water removal in fuel cells by capillary droplet actuation. *Sens. Actuat. A* **2008**, *143*, 49-57.

205. Min, C.H. Performance of a proton exchange membrane fuel cell with a stepped flow field design. *J. Power Sources* **2009**, *186*, 370-376.

206. Yi, J.S.; Yang, J.D.; King, C. Water management along the flow channels of PEM fuel cells. *AIChE J.* **2004**, *50*, 2594-2603.

207. Ge, S.H.; Li, X.G.; Hsing, I.M. Internally humidified polymer electrolyte fuel cells using water absorbing sponge. *Electrochim. Acta* **2005**, *50*, 1909-1916.

208. Ge, S.H.; Li, X.G.; Hsing, I.M. Water management in PEMFCs using absorbent wicks. *J. Electrochem. Soc.* **2004**, *151*, B523-B528.

209. Buie, C.R.; Posner, J.D.; Fabian, T.; Cha, S.W.; Kim, D.; Prinz, F.B.; Eaton, J.K.; Santiago, J.G. Water management in proton exchange membrane fuel cells using integrated electroosmotic pumping. *J. Power Sources* **2006**, *161*, 191-202.

210. Strickland, D.G.; Litster, S.; Santiago, J.G. Current distribution in polymer electrolyte membrane fuel cell with active water management. *J. Power Sources* **2007**, *174*, 272-281.

211. Litster, S.; Buie, C.R.; Fabian, T.; Eaton, J.K.; Santiago, J.G. Active water management for PEM fuel cells. *J. Electrochem. Soc.* **2007**, *154*, B1049-B1058.

212. Hogarth, W.; Benziger, J.B. Operation of polymer electrolyte membrane fuel cells with dry feeds: Design and operating strategies. *J. Power Sources* **2006**, *159*, 968-978.

213. Wilkinson, D.P.; Voss, H.H.; Prater, K. Water management and stack design for solid polymer fuel cells. *J. Power Sources* **1994**, *49*, 117-127.

214. Freire, T.J.P.; Gonzalz, E.R. Effect of membrane characteristics and humidification conditions on the impedance response of polymer electrolyte fuel cells. *J. Electroanal. Chem.* **2001**, *503*, 57-68.

215. Watanabe, M.; Satoh, Y.; Shimura, C. Management of the water content in polymer electrolyte membranes with porous fiber wicks. *J. Electrochem. Soc.* **1993**, *140*, 3190-3193.

216. Watanabe, M.; Uchida, H.; Seki, Y.; Emori, M. Self-humidifying polymer electrolyte membranes for fuel cells. *J. Electrochem. Soc.* **1996**, *143*, 3847-3852.

217. Pereira, F.; Vallé, K.; Belleville, P.; Morin, A.; Lambert, S.; Sanchez, C. Advanced mesostructured hybrid silica-nafion membranes for high-performance PEM fuel cell. *Chem. Mater.* **2008**, *20*, 1710-1718.

218. Mistry, M.K.; Choudhury, N.R.; Dutta, N.K.; Knott, R.; Shi, Z.Q.; Holdcroft, S. Novel organic-inorganic hybrids with increased water retention for elevated temperature proton exchange membrane application. *Chem. Mater.* **2008**, *20*, 6857-6870.

219. McKeen, J.C.; Yan, Y.S.; Davis, M.E. Proton conductivity of acid-functionalized zeolite beta, MCM-41, and MCM-48: Effect of acid strength. *Chem. Mater.* **2008**, *20*, 5122-5124.

220. Adjemian, K.T.; Dominey, R.; Krishnan, L.; Ota, H.; Majsztrik, P.; Zhang, T.; Mann, J.; Kirby, B.; Gatto, L.; Velo-Simpson, M.; Leahy, J.; Srinivasan, S.; Benziger, J.B.; Bocarsly, A.B. Function and characterization of metal oxide-nafion composite membranes for elevated-temperature H_2/O_2 PEM fuel cells. *Chem. Mater.* **2006**, *18*, 2238-2248.

221. Persson, J.C.; Jannasch, P. Self-conducting benzimidazole oligomers for proton transport. *Chem. Mater.* **2003**, *15*, 3044-3045.

222. Li, Q.F.; He, R.H.; Jensen, J.O.; Bjerrum, N.J. Approaches and recent development of polymer electrolyte membranes for fuel cells operating above 100 ℃. *Chem. Mater.* **2003**, *15*, 4896-4915.

223. Bevers, D.; Rogers, R.; von Bradke, M. Examination of the influence of PTFE coating on the properties of carbon paper in polymer electrolyte fuel cells. *J. Power Sources* **1996**, *63*, 193-201.

224. Lin, G.Y.; Nguyen, T.V. Effect of thickness and hydrophobic polymer content of the gas diffusion layer on electrode flooding level in a PEMFC. *J. Electrochem. Soc.* **2005**, *152*, A1942-A1948.

225. Williams, M.V.; Kunz, H.R.; Fenton, J.M. Opertation of Nafion®-based PEM fuel cells with no external humidification: influence of opertating conditions and gas diffusion layers. *J. Power Sources* **2004**, *135*, 122-134.

226. Escribano, S.; Blachot, J.F.; Ethève, J.; Morin, A.; Mosdale, R. Characterization of PEMFCs gas diffusion layers properties. *J. Power Sources* **2006**, *156*, 8-13.

227. Ralph, T.R.; Hards, G.A.; Keating, J.E.; Campbell, S.A.; Wilkinson, D.P.; Davis, M.; St-Pierre, J.; Johnson, M.C. Low cost electrodes for proton exchange membrane fuel cells. *J. Electrochem. Soc.* **1997**, *144*, 3845-3857.

228. Park, G.G.; Sohn, Y.J.; Yang, T.H.; Yoon, Y.G.; Lee, W.Y.; Kim, C.S. Effect of PTFE contents in the gas diffusion media on the performance of PEMFC. *J. Power Sources* **2004**, *131*, 182-187.

229. Atiyeh, H.K.; Karan, K.; Peppley, B.; Phoenix, A.; Halliop, E.; Pharoah, J. Experimental investigation of the role of a microporous layer on the water transport and performance of a PEM fuel cell. *J. Power Sources* **2007**, *170*, 111-121.

230. Velayutham, G.; Kaushik, J.; Rajalakshmi, N.; Dhathathreyan, K.S. Effect of PTFE content in gas diffusion media and microlayer on the performance of PEMFC tested under ambient pressure. *Fuel Cells* **2007**, *7*, 314-318.

231. Qi, Z.G.; Kaufman, A. Improvement of water management by a microporous sublayer for PEM fuel cells. *J. Power Sources* **2002**, *109*, 38-46.

232. Giorgi, L.; Antolini, E.; Pozio, A.; Passalacqua, E. Influence of the PTFE content in the diffusion layer of low-Pt loading electrodes for polymer electrolyte fuel cells. *Electrochim. Acta* **1998**, *43*, 3675-3680.

233. Lufrano, F.; Passalacqua, E.; Squadrito, G.; Patti, A.; Giorgi, L. Improvement in the diffusion characteristics of low Pt-loaded electrodes for PEFCs. *J. Appl. Electrochem.* **1999**, *29*, 445-448.

234. Moreira, J.; Ocampo, A.L.; Sebastian, P.J.; Smit, M.A.; Salazar, M.D.; del Angel, P.; Montoya, J.A.; Pérez, R.; Martínez, L. Influence of the hydrophobic material content in the gas diffusion electrodes on the performance of a PEM fuel cell. *Int. J. Hydrogen Energy* **2003**, *28*, 625-627.

235. Kong, C.S.; Kim, D.Y.; Lee, H.K.; Shul, Y.G.; Lee, T.H. Influence of pore-size distribution of diffusion layer on mass-transport problems of proton exchange membrane fuel cells. *J. Power Sources* **2002**, *108*, 185-191.

236. Chu, H.S.; Yeh, C.; Chen, F. Effects of porosity changes of gas diffuser on performance of proton exchange membrane fuel cell. *J. Power Sources* **2003**, *123*, 1-9.

237. Lee, H.K.; Park, J.H.; Kim, D.Y.; Lee, T.H. A study on the characteristics of the diffusion layer thickness and porosity of the PEMFC. *J. Power Sources* **2004**, *131*, 200-206.

238. Wang, E.D.; Shi, P.F.; Du, C.Y. Treatment and characterization of gas diffusion layers by sucrose carbonization for PEMFC applications. *Electrochem. Commun.* **2008**, *10*, 555-558.

239. Jiao, K.; Zhou, B. Innovative gas diffusion layers and their water removal characteristics in PEM fuel cell cathode. *J. Power Sources* **2007**, *169*, 296-314.

240. Zhang, F.Y.; Advani, S.G.; Prasad, A.K. Performance of a metallic gas diffusion layer for PEM fuel cells. *J. Power Sources* **2008**, *176*, 293-298.

241. Jordan, L.R.; Shukla, A.K.; Behrsing, T.; Avery, N.R.; Muddle, B.C.; Forsyth, M. Effect of diffusion-layer morphology on the performance of polymer electrolyte fuel cells operating at atmospheric pressure. *J. Appl. Electrochem.* **2000**, *30*, 641-646.

242. Antolini, E.; Passos, R.R.; Ticianelli, E.A. Effects of the cathode gas diffusion layer characteristics on the performance of polymer electrolyte fuel cells. *J. Appl. Electrochem.* **2002**, *32*, 383-388.

243. Pasaogullari, U.; Wang, C.Y. Two-phase transport and the role of micro-porous layer in polymer electrolyte fuel cells. *Electrochim. Acta* **2004**, *49*, 4359-4369.

244. Pasaogullari, U.; Wang, C.Y.; Chen, K.S. Two-phase transport in polymer electrolyte fuel cells with bi-layer cathode gas diffusion media. *J. Electrochem. Soc.* **2005**, *152*, A1574-A1582.

245. Weber, A.Z.; Newman, J. Effects of microporous layers in polymer electrolyte fuel cells. *J. Electrochem. Soc.* **2005**, *152*, A677-A688.

246. Lin, G.Y.; Nguyen, T.V. A two-dimensional two-phase model of a PEM fuel cell. *J. Electrochem. Soc.* **2006**, *153*, A372-A382.

247. Paganin, V.A.; Ticianelli, E.A.; Gonzalez, E.R. Development and electrochemical studies of gas diffusion electrodes for polymer electrolyte fuel cells. *J. Appl. Electrochem.* **1996**, *26*, 297-304.

248. Song, J.M.; Cha, S.Y.; Lee, W.M. Optimal composition of polymer electrolyte fuel cell electrodes determined by the AC impedance method. *J. Power Sources* **2001**, *94*, 78-84.

249. Choi, K.H.; Peck, D.H.; Kim, C.S.; Shin, D.R.; Lee, T.H. Water transport in polymer membranes for PEMFC. *J. Power Sources* **2000**, *86*, 197-201.

250. Chen, J.; Matsuura, T.; Hori, M. Novel gas diffusion layer with water management function for PEMFC. *J. Power Sources* **2004**, *131*, 155-161.

251. Yan, Q.; Toghiani, H.; Wu, J. Investigation of water transport through membrane in a PEM fuel cell by water balance experiments. *J. Power Sources* **2006**, *158*, 316-325.

252. Cai, Y.H.; Hu, J.; Ma, H.P.; Yi, B.L.; Zhang, H.M. Effect of water transport properties on a PEM fuel cell operating with dry hydrogen. *Electrochim. Acta* **2006**, *51*, 6361-6366.

253. Wang, X.L.; Zhang, H.M.; Zhang, J.L.; Xu, H.F.; Tian, Z.Q.; Chen, J.; Zhong, H.X.; Liang, Y.M.; Yi, B.L. Micro-porous layer with composite carbon black for PEM fuel cells. *Electrochim. Acta* **2006**, *51*, 4909-4915.

254. Park, S.; Lee, J.W.; Popov, B.N. Effect of carbon loading in microporous layer on PEM fuel cell performance. *J. Power Sources* **2006**, *163*, 357-363.

255. Yu, J.R.; Yoshikawa, Y.; Matsuura, T.; Islam, M.N.; Hroi, M. Preparing gas-diffusion layers of PEMFCs with a dry deposition technique. *Electrochem. Solid-State Lett.* **2005**, *8*, A152-A155.

256. Gostick, J.T.; Ioannidis, M.A.; Fowler, M.W.; Pritzker, M.D. On the role of the microporous layer in PEMFC operation. *Electrochem. Commun.* **2009**, *11*, 576-579.

257. Holmström, N.; Ihonen, J.; Lundblad, A.; Lindbergh, G. The influence of the gas diffusion layer on water management in polymer electrolyte fuel cells. *Fuel Cells* **2007**, *7*, 306-313.

258. Ramasamy, R.P.; Kumbur, E.C.; Mench, M.M.; Liu, W.; Moore, D.; Murthy, M. Investigation of macro- and micro-porous layer interaction in polymer electrolyte fuel cells. *Int. J. Hydrogen Energy* **2008**, *33*, 3351-3367.

259. Park, S.; Lee, J.W.; Popov, B.N. Effect of PTFE content in microporous layer on water management in PEM fuel cells. *J. Power Sources* **2008**, *177*, 457-463.

260. Nakajima, H.; Konomi, T.; Kitahara, T. Direct water balance analysis on a polymer electrolyte fuel cell (PEFC): Effects of hydrophobic treatment and microporous layer addition to the gas diffusion layer of PEFC on its performance during a simulated start-up operation. *J. Power Sources* **2007**, *171*, 457-463.

261. Ihonen, J.; Mikkola, M.; Lindbergh, G. Flooding of gas diffusion backing in PEFCs. *J. Electrochem. Soc.* **2004**, *151*, A1152-A1161.

262. Yan, W.M.; Hsueh, C.Y.; Soong, C.Y.; Chen, F.L.; Cheng, C.H.; Mei, S.C. Effects of fabrication processes and material parameters of GDL on cell performance of PEM fuel cell. *Int. J. Hydrogen Energy* **2007**, *32*, 4452-4458.

263. Park, G.G.; Sohn, Y.J.; Yim, S.D.; Yang, T.H.; Yoon, Y.G.; Lee, W.Y.; Eguchi, K.; Kim, C.S. Adoption of nano-materials for the micro-layer in gas diffusion layers of PEMFCs. *J. Power Sources* **2006**, *163*, 113-118.

264. Yoshikawa, Y.; Matsuura, T.; Kato, M.; Hori, M. Design of low-humidification PEMFC by using cell simulator and its power generation verification test. *J. Power Sources* **2006**, *158*, 143-147.

265. Shi, J.S.; Tian, J.H.; Zhang, C.; Shan, Z.Q. A novel method for the preparation of a PEMFC water management layer. *J. Power Sources* **2006**, *164*, 284-286.

266. Chen, J.H.; Matsuura, T.; Hori, M. Novel gas diffusion layer with water management functions for PEMFC. *J. Power Sources* **2004**, *131*, 155-161.

267. Tian, J.H.; Shi, Z.Y.; Shi, J.S.; Shan, Z.Q. Preparation of water management layer and effects of its composition on performance of PEMFCs. *Energy Convers Manage* **2008**, *49*, 1500-1505.

268. Wang, E.D.; Shi, P.F.; Du, C.Y. A novel self-humidifying membrane electrode assembly with water transfer region for proton exchange membrane fuel cells. *J. Power Sources* **2008**, *175*, 183-188.

269. Eikerling, M.; Kornyshev, A.A. Modelling the performance of the cathode catalyst layer of polymer electrolyte fuel cells. *J. Electroanal. Chem.* **1998**, *453*, 89-106.

270. Nguyen, T.V.; Natarajan, D.; Jain, R. Optimized catalyst layer structure for PEM fuel cells. *ECS Trans.* **2006**, *1*, 501-508.

271. Okada, T.; Wakayama, N.I.; Wang, L.B.; Shingu, H.; Okano, J.; Ozawa, T. The effect of magnetic field on the oxygen reduction reaction and its application in polymer electrolyte fuel cells. *Electrochim. Acta* **2003**, *48*, 531-539.

272. Wang, L.B.; Wakayama, N.I.; Okada, T. Numerical simulation of a new water management for PEM fuel cell using magnet particles deposited in the cathode side catalyst layer. *Electrochem. Commun.* **2002**, *4*, 584-588.

273. Wei, Z.D.; Ji, M.B.; Chen, S.G.; Li, L. An ordered anti-flooding gas porous electrode. *Chinese Invention Patent: CN 200810069270.2*, 2008.

274. Wei, Z.D.; Ji, M.B.; Chen, S.G.; Li, L. An anti-flooding gas porous electrode used in alkaline. *Chinese Invention Patent: CN 200810069274.0*, 2008.

275. Ji, M.B.; Wei, Z.D.; Chen, S.G.; Qi, X.Q.; Li, L.; Zhang, Q.; Liao, C.; Tang, R. A novel anode for preventing liquid sealing effect in DMFC. *Int. J. Hydrogen Energ.* **2009**, *34*, 2765-2770.

276. Wei, Z.D.; Ji, M.B.; Chen, S.G.; Li, L. An anode for preventing liquid sealing effect in DMFC. *Chinese Invention Patent: CN 200810233093.7*, 2008.